The three- and four-Higgs couplings in the general two-Higgs-doublet model

D. Jurčiukonis[a] and L. Lavoura[b]

[a]*Institute of Theoretical Physics and Astronomy, University of Vilnius,*
Saulėtekio ave. 3, LT-10222 Vilnius, Lithuania

[b]*Instituto Superior Técnico, CFTP, Universidade de Lisboa,*
1049-001 Lisboa, Portugal

E-mail: darius.jurciukonis@tfai.vu.lt, balio@cftp.tecnico.ulisboa.pt

Abstract: We apply the unitarity bounds and the bounded-from-below (BFB) bounds to the most general scalar potential of the two-Higgs-doublet model (2HDM). We do this in the Higgs basis, i.e. in the basis for the scalar doublets where only one doublet has vacuum expectation value. In this way we obtain bounds on the scalar masses and couplings that are valid for all 2HDMs. We compare those bounds to the analogous bounds that we have obtained for other simple extensions of the Standard Model (SM), namely the 2HDM extended by one scalar singlet and the extension of the SM through two scalar singlets.

Contents

1 Introduction

In order to unveil the detailed mechanism of electroweak symmetry breaking it is crucial to measure the self-couplings of the boson with mass 125 GeV discovered in 2012 at the LHC [1, 2]. In this paper we call that boson h_1. The Standard Model (SM) predicts h_1 to be a scalar and predicts its cubic and quartic couplings g_3 and g_4, which we define through

$$\mathcal{L} = \cdots - g_3 \left(h_1 \right)^3 - g_4 \left(h_1 \right)^4 , \tag{1.1}$$

to be $g_3^{\mathrm{SM}} \approx 32\,\mathrm{GeV}$ and $g_4^{\mathrm{SM}} \approx 0.032$, respectively. However, in Nature the scalar sector may be more complicated than in the SM [3] and then g_3 and g_4 might have very different values. In this paper we survey the allowed values of g_3 and g_4 in three extensions of the SM:

- The SM plus two real, neutral scalar singlets and with a reflection symmetry on each of those singlets. Let SM2S denote this model, which we treat in section 2.

- The two-Higgs-doublet model (2HDM), which is the focus object of section 3.

- The 2HDM with the addition of one real, neutral scalar singlet and with a reflection symmetry of that singlet. This model, which we dubb the 2HDM1S, is dealt with in section 4.

Our ingredients for bounding g_3 and g_4 in each of these models are:

- The bounded-from-below (BFB) and the unitarity conditions on the quartic part of the scalar potential of each model. We apply those conditions directly in the basis for the scalar doublets where only one of them has vacuum expectation value (VEV).

- The experimental bound on the oblique parameter T [4].

- The (approximate) bound $\cos\vartheta > 0.9$ on the h_1 component $\cos\vartheta$ of the scalar doublet with nonzero VEV.

Other authors before us [5]–[9–12] have used the BFB and unitarity constraints in order to bound the scalar masses and couplings of the 2HDM. However, they have done it in the context of a constrained version of the model, viz. the 2HDM with a reflection symmetry acting on one of the scalar doublets, leading to $\lambda_6 = \lambda_7 = 0$ in the scalar potential of equation (3.1). In this paper we deal on the fully general 2HDM. We enforce the BFB and unitarity constraints in the so-called Higgs basis, i.e. the basis where only one of the doublets has VEV. Since that basis exists for every 2HDM, we thus obtain results that apply to every 2HDM.

At present there are only indirect, very rough bounds on g_3. Using the Standard Model Effective Theory developed in refs. [13, 14] and experimental data [15], ref. [16] has found that $-8.4 < g_3/g_3^{\mathrm{SM}} < 13.4$. From the contribution of g_3 to the oblique parameters S and T, ref. [17] derived $-14.0 < g_3/g_3^{\mathrm{SM}} < 17.4$. The authors of ref. [18] obtained firstly $-9.4 < g_3/g_3^{\mathrm{SM}} < 17.0$ and then [19] $-8.2 < g_3/g_3^{\mathrm{SM}} < 13.7$. The partial-wave unitarity of $h_1 h_1 \to h_1 h_1$ scattering has been used [20] to obtain $\left| g_3/g_3^{\mathrm{SM}} \right| \lesssim 6.5$ and $\left| g_4/g_4^{\mathrm{SM}} \right| \lesssim 65$. In an analysis of a specific three-Higgs-doublet model, ref. [21] has found that in that model $-1.3 < g_3/g_3^{\mathrm{SM}} < 20.0$ and $1.05 < g_4/g_4^{\mathrm{SM}} < 1.6$.

The measurement of g_3 should be possible at future colliders, and may even eventually become possible at the LHC [22, 23]. Reference [24] concluded that one may be able to measure g_3 provided $-0.72 < g_3/g_3^{\mathrm{SM}} < 7.05$. Unfortunately, measuring g_4 is probably more challenging [25, 26].

1.1 g_3 and g_4 in the SM

The Standard Model has only one scalar doublet ϕ_1. We write it

$$\phi_1 = \begin{pmatrix} G^+ \\ v + \left(H + iG^0 \right)/\sqrt{2} \end{pmatrix}, \tag{1.2}$$

where v is the VEV, which is real and positive, and G^+ and G^0 are (unphysical) Goldstone bosons. In the SM H coincides with the observed scalar h_1. The scalar potential is

$$V = \mu_1 \phi_1^\dagger \phi_1 + \frac{\lambda_1}{2} \left(\phi_1^\dagger \phi_1 \right)^2. \tag{1.3}$$

The minimization condition of V is $\mu_1 = -\lambda_1 v^2$. Therefore, in the unitary gauge where $G^\pm$ and G^0 do not exist,

$$V = -\frac{\lambda_1 v^4}{2} + \lambda_1 v^2 H^2 + \frac{\lambda_1 v}{\sqrt{2}} H^3 + \frac{\lambda_1}{8} H^4. \tag{1.4}$$

The second term in the right-hand side of equation (1.4) indicates that the squared mass M_1 of the observed scalar is given by $M_1 = 2\lambda_1 v^2$. Therefore,

$$V = -\frac{M_1 v^2}{4} + \frac{M_1}{2} \left(h_1 \right)^2 + \frac{M_1}{2\sqrt{2}v} \left(h_1 \right)^3 + \frac{M_1}{16 v^2} \left(h_1 \right)^4 \tag{1.5a}$$

$$= \cdots + g_3^{\text{SM}} \left(h_1 \right)^3 + g_4^{\text{SM}} \left(h_1 \right)^4. \tag{1.5b}$$

Using the approximate experimental values

$$M_1 = \left(125\,\text{GeV} \right)^2, \tag{1.6a}$$

$$v = 174\,\text{GeV}, \tag{1.6b}$$

one gathers from equation (1.5a) that

$$g_3^{\text{SM}} = \frac{M_1}{2\sqrt{2}v} = 31.7\,\text{GeV}, \tag{1.7a}$$

$$g_4^{\text{SM}} = \frac{M_1}{16 v^2} = 0.0323. \tag{1.7b}$$

It should be noted that the sign of g_3 implicitly depends on the sign of h_1. We fix that sign by noting that the covariant derivative of ϕ_1 gives rise to a term

$$\mathcal{L} = \cdots + \frac{g^2}{2} W_\mu^+ W^{\mu-} \left(v + \frac{H}{\sqrt{2}} \right)^2 \tag{1.8a}$$

$$= \cdots + \frac{g^2 v}{\sqrt{2}} W_\mu^+ W^{\mu-} H. \tag{1.8b}$$

Thus, the coupling $W_\mu^+ W^{\mu-} h_1$, viz. $g^2 v / \sqrt{2}$, is positive.

2 The Standard Model plus two singlets

We consider the Standard Model with the addition of two real $SU(2) \times U(1)$-invariant scalar fields S_1 and S_2.[1] We assume two symmetries $S_1 \to -S_1$ and $S_2 \to -S_2$. We call this model the SM2S.[2] The scalar potential is

$$V = V_2 + V_4, \tag{2.1a}$$

$$V_2 = \mu_1 \phi_1^\dagger \phi_1 + m_1^2 S_1^2 + m_2^2 S_2^2, \tag{2.1b}$$

$$V_4 = \frac{\lambda_1}{2} \left(\phi_1^\dagger \phi_1\right)^2 + \frac{\psi_1}{2} S_1^4 + \frac{\psi_2}{2} S_2^4 + \psi_3 S_1^2 S_2^2 + \phi_1^\dagger \phi_1 \left(\xi_1 S_1^2 + \xi_2 S_2^2\right). \tag{2.1c}$$

2.1 Unitarity condidions

We derive the unitarity conditions on the parameters of V_4.[3] We follow closely the method of ref. [33]. We write

$$\phi_1 = \begin{pmatrix} a \\ b \end{pmatrix}, \quad \phi_1^\dagger = \begin{pmatrix} a^* & b^* \end{pmatrix}, \quad S_1^* = S_1, \quad S_2^* = S_2, \tag{2.2}$$

where a and b are complex fields. Then,

$$V_4 = \frac{\lambda_1}{2} \left(a^* a^* a a + b^* b^* b b + 2 a^* b^* a b\right) + \frac{\psi_1}{2} S_1^4 + \frac{\psi_2}{2} S_2^4 + \psi_3 S_1^2 S_2^2 \tag{2.3a}$$

$$+ \left(a^* a + b^* b\right) \left(\xi_1 S_1^2 + \xi_2 S_2^2\right). \tag{2.3b}$$

There are seven two-particle scattering channels (Q is the electric charge, T_3 is the third component of weak isospin):

1. The channel $Q = 2$, $T_3 = 1$, with one state aa.

2. The channel $Q = 0$, $T_3 = -1$, with one state bb.

3. The channel $Q = 1$, $T_3 = 0$, with one state ab.

4. The channel $Q = 1$, $T_3 = 1$, with one state ab^*.

5. The channel $Q = 1$, $T_3 = 1/2$, with two states aS_1 and aS_2.

6. The channel $Q = 0$, $T_3 = -1/2$, with two states bS_1 and bS_2.

7. The channel $Q = 0$, $T_3 = 0$, with five states S_1^2, S_2^2, $S_1 S_2$, $a^* a$, and $b^* b$.

---

[1]In appendix A we treat the simpler case of the HSM, viz. the Standard Model with the addition of *only one* real gauge singlet.

[2]The SM2S has already been mentioned in the literature as a model for Dark Matter, see refs. [27–30].

[3]Strictly speaking, the unitarity conditions derived and utilized in this paper are the ones valid in the limit of infinite Mandelstam parameter s. For finite s one must take into account the trilinear vertices that are induced from the quartic vertices when one substitutes one of the fields by its VEV. The unitarity conditions then become s-dependent and may be either more or less restrictive than the conditions in the limit of infinite s. See refs. [31, 32].

In order to derive the unitarity conditions one must write the scattering matrices for pairs of one incoming state and one outgoing state with the same Q and T_3. Let the incoming state be xy and let the outgoing state by zw, where x, y, z, and w may be either a, a^*, b, b^*, S_1, or S_2. The corresponding entry in the scattering matrix is the coefficient of xyz^*w^* in V_4, with the following additions:

For each n identical operators in xyz^*w^* there is an additional factor $n!$ in the entry.

If $x = y$ there is additional factor $2^{-1/2}$ in the entry.

If $z = w$ there is additional factor $2^{-1/2}$ in the entry.

One finds in this way that the scattering matrices for the channels 1, 2, 3, and 4 are

$$\begin{pmatrix} \lambda_1 \end{pmatrix}. \tag{2.4}$$

The scattering matrices for the channels 5 and 6 are

$$\begin{pmatrix} 2\xi_1 & 0 \\ 0 & 2\xi_2 \end{pmatrix}. \tag{2.5}$$

The scattering matrix for channel 7 is

$$\begin{pmatrix} 6\psi_1 & 2\psi_3 & 0 & \sqrt{2}\xi_1 & \sqrt{2}\xi_1 \\ 2\psi_3 & 6\psi_2 & 0 & \sqrt{2}\xi_2 & \sqrt{2}\xi_2 \\ 0 & 0 & 4\psi_3 & 0 & 0 \\ \sqrt{2}\xi_1 & \sqrt{2}\xi_2 & 0 & 2\lambda_1 & \lambda_1 \\ \sqrt{2}\xi_1 & \sqrt{2}\xi_2 & 0 & \lambda_1 & 2\lambda_1 \end{pmatrix}. \tag{2.6}$$

The matrix (2.6) is similar to the matrix

$$\begin{pmatrix} 6\psi_1 & 2\psi_3 & 2\xi_1 & 0 & 0 \\ 2\psi_3 & 6\psi_2 & 2\xi_2 & 0 & 0 \\ 2\xi_1 & 2\xi_2 & 3\lambda_1 & 0 & 0 \\ 0 & 0 & 0 & 4\psi_3 & 0 \\ 0 & 0 & 0 & 0 & \lambda_1 \end{pmatrix}. \tag{2.7}$$

The unitarity conditions are the following: the eigenvalues of all the scattering matrices should be smaller, in modulus, than 4π. Thus, in our case,

$$|\lambda_1| < 4\pi, \tag{2.8a}$$

$$|\xi_1| < 2\pi, \tag{2.8b}$$

$$|\xi_2| < 2\pi, \tag{2.8c}$$

$$|\psi_3| < \pi, \tag{2.8d}$$

and the eigenvalues of

$$\begin{pmatrix} 6\psi_1 & 2\psi_3 & 2\xi_1 \\ 2\psi_3 & 6\psi_2 & 2\xi_2 \\ 2\xi_1 & 2\xi_2 & 3\lambda_1 \end{pmatrix} \tag{2.9}$$

should have moduli smaller than 4π.

2.2 Bounded-from-below conditions

One may write

$$V_4 = \frac{1}{2} \begin{pmatrix} X & Y & Z \end{pmatrix} \begin{pmatrix} \lambda_1 & \xi_1 & \xi_2 \\ \xi_1 & \psi_1 & \psi_3 \\ \xi_2 & \psi_3 & \psi_2 \end{pmatrix} \begin{pmatrix} X \\ Y \\ Z \end{pmatrix} \tag{2.10}$$

where $X = \phi_1^\dagger \phi_1$, $Y = S_1^2$, and $Z = S_2^2$ are positive definite quantities independent of each other. In order for V_4 to be positive the square matrix in equation (2.10) must be *copositive* [34]. A real symmetric matrix M is copositive if $x^T M x > 0$ for any vector x with non-negative components. A necessary condition for a real $n \times n$ matrix to be copositive is that all its $(n-1) \times (n-1)$ principal submatrices are copositive too.[4] Thus, the matrices

$$\begin{pmatrix} \lambda_1 \end{pmatrix}, \quad \begin{pmatrix} \psi_1 \end{pmatrix}, \quad \begin{pmatrix} \psi_2 \end{pmatrix}, \quad \begin{pmatrix} \lambda_1 & \xi_1 \\ \xi_1 & \psi_1 \end{pmatrix}, \quad \begin{pmatrix} \lambda_1 & \xi_2 \\ \xi_2 & \psi_2 \end{pmatrix}, \quad \begin{pmatrix} \psi_1 & \psi_3 \\ \psi_3 & \psi_2 \end{pmatrix} \tag{2.11}$$

must be copositive. A real 1×1 matrix $\begin{pmatrix} a \end{pmatrix}$ is copositive if $a > 0$; a real 2×2 matrix $\begin{pmatrix} a & c \\ c & b \end{pmatrix}$ is copositive if $a > 0$, $b > 0$, and $c > -\sqrt{ab}$. This leads to the six necessary BFB conditions

$$\lambda_1 > 0, \tag{2.12a}$$

$$\psi_1 > 0, \tag{2.12b}$$

$$\psi_2 > 0, \tag{2.12c}$$

$$a_1 \equiv \xi_1 + \sqrt{\lambda_1 \psi_1} > 0, \tag{2.12d}$$

$$a_2 \equiv \xi_2 + \sqrt{\lambda_1 \psi_2} > 0, \tag{2.12e}$$

$$a_3 \equiv \psi_3 + \sqrt{\psi_1 \psi_2} > 0. \tag{2.12f}$$

In order for the full 3×3 matrix in equation (2.10) to be copositive an additional BFB condition is required [35]:

$$\sqrt{\lambda_1 \psi_1 \psi_2} + \xi_1 \sqrt{\psi_2} + \xi_2 \sqrt{\psi_1} + \psi_3 \sqrt{\lambda_1} + \sqrt{2 a_1 a_2 a_3} > 0. \tag{2.13}$$

2.3 Procedure

Let the VEV of S_1 be w_1 and let the VEV of S_2 be w_2.[5] Then, the vacuum stability conditions are

$$\mu_1 = -\lambda_1 v^2 - \xi_1 w_1^2 - \xi_2 w_2^2, \tag{2.14a}$$

$$m_1^2 = -\psi_1 w_1^2 - \psi_3 w_2^2 - \xi_1 v^2, \tag{2.14b}$$

$$m_2^2 = -\psi_2 w_2^2 - \psi_3 w_1^2 - \xi_2 v^2. \tag{2.14c}$$

---

[4]The principal submatrices are obtained by deleting rows and columns of the original matrix in a symmetric way, i.e. when one deletes the $i_1, i_2, \ldots, i_k$ rows one also deletes the $i_1, i_2, \ldots, i_k$ columns.

[5]In appendix B we demonstrate that stability points of the potential with either $w_1 = 0$ or $w_2 = 0$ have a higher value of the potential and cannot therefore be the vacuum.

Using equation (1.2) with $G^+ = 0$ and $G^0 = 0$, i.e. in the unitary gauge, together with $S_1 = w_1 + \sigma_1$ and $S_2 = w_2 + \sigma_2$, one obtains

$$V = -\frac{\lambda_1}{2} v^4 - \frac{\psi_1}{2} w_1^4 - \frac{\psi_2}{2} w_2^4 - \psi_3 w_1^2 w_2^2 - v^2 \left(\xi_1 w_1^2 + \xi_2 w_2^2 \right) \tag{2.15a}$$

$$+ \frac{1}{2} \left(H \ \sigma_1 \ \sigma_2 \right) M \begin{pmatrix} H \\ \sigma_1 \\ \sigma_2 \end{pmatrix} \tag{2.15b}$$

$$+ \frac{\lambda_1 v}{\sqrt{2}} H^3 + 2\psi_1 w_1 \sigma_1^3 + 2\psi_2 w_2 \sigma_2^3 \tag{2.15c}$$

$$+ \xi_1 H \sigma_1 \left(\sqrt{2} v \sigma_1 + w_1 H \right) + \xi_2 H \sigma_2 \left(\sqrt{2} v \sigma_2 + w_2 H \right) \tag{2.15d}$$

$$+ 2\psi_3 \sigma_1 \sigma_2 \left(w_1 \sigma_2 + w_2 \sigma_1 \right) \tag{2.15e}$$

$$+ \frac{\lambda_1}{8} H^4 + \frac{\psi_1}{2} \sigma_1^4 + \frac{\psi_2}{2} \sigma_2^4 + \frac{\xi_1}{2} H^2 \sigma_1^2 + \frac{\xi_2}{2} H^2 \sigma_2^2 + \psi_3 \sigma_1^2 \sigma_2^2, \tag{2.15f}$$

where

$$M = 2 \begin{pmatrix} \lambda_1 v^2 & \sqrt{2} \xi_1 v w_1 & \sqrt{2} \xi_2 v w_2 \\ \sqrt{2} \xi_1 v w_1 & 2\psi_1 w_1^2 & 2\psi_3 w_1 w_2 \\ \sqrt{2} \xi_2 v w_2 & 2\psi_3 w_1 w_2 & 2\psi_2 w_2^2 \end{pmatrix}. \tag{2.16}$$

One diagonalizes the real symmetric matrix M as

$$M = R^T \, \text{diag} \left(M_1, \ M_2, \ M_3 \right) R, \tag{2.17}$$

where R is a 3×3 orthogonal matrix that may be parameterized as

$$R = \begin{pmatrix} c_1 & s_1 c_3 & s_1 s_3 \\ -s_1 c_2 & c_1 c_2 c_3 + s_2 s_3 & c_1 c_2 s_3 - s_2 c_3 \\ -s_1 s_2 & c_1 s_2 c_3 - c_2 s_3 & c_1 s_2 s_3 + c_2 c_3 \end{pmatrix}. \tag{2.18}$$

Here, $c_j = \cos \vartheta_j$ and $s_j = \sin \vartheta_j$ for $j = 1, 2, 3$. One has

$$\begin{pmatrix} H \\ \sigma_1 \\ \sigma_2 \end{pmatrix} = R^T \begin{pmatrix} h_1 \\ h_2 \\ h_3 \end{pmatrix}, \tag{2.19}$$

where the h_j are the physical scalars, i.e. the eigenstates of mass; the scalar h_j has squared mass M_j. We assume that h_1 is the already-observed scalar. The interactions of the scalars with $W^+ W^-$ are given by equation (1.8b), i.e.

$$\mathcal{L} = \cdots + \frac{g^2 v}{\sqrt{2}} W_\mu^- W^{\mu+} \left(c_1 h_1 - s_1 c_2 h_2 - s_1 s_2 h_3 \right). \tag{2.20}$$

We define the sign of the field h_1 to be such that the coupling of h_1 to $W^+ W^-$ has the same sign as in the Standard Model. Thus, we choose $-\pi/2 < \vartheta_1 < \pi/2$.

According to equation (2.15),

$$g_3 = \frac{\lambda_1 v}{\sqrt{2}} c_1^3 + 2\psi_1 w_1 s_1^3 c_3^3 + 2\psi_2 w_2 s_1^3 s_3^3 \tag{2.21a}$$

$$+ \xi_1 c_1 s_1 c_3 \left(\sqrt{2} v s_1 c_3 + w_1 c_1 \right) + \xi_2 c_1 s_1 s_3 \left(\sqrt{2} v s_1 s_3 + w_2 c_1 \right) \tag{2.21b}$$

$$+ 2\psi_3 s_1^3 c_3 s_3 \left(w_1 s_3 + w_2 c_3 \right) \tag{2.21c}$$

$$= \frac{M_1}{2\sqrt{2} v} \left(c_1^3 + \frac{\sqrt{2} v}{w_1} s_1^3 c_3^3 + \frac{\sqrt{2} v}{w_2} s_1^3 s_3^3 \right) \tag{2.21d}$$

$$= g_3^{\text{SM}} \left(c_1^3 + \frac{\sqrt{2} v}{w_1} s_1^3 c_3^3 + \frac{\sqrt{2} v}{w_2} s_1^3 s_3^3 \right), \tag{2.21e}$$

and

$$g_4 = \frac{\lambda_1}{8} c_1^4 + \frac{\psi_1}{2} s_1^4 c_3^4 + \frac{\psi_2}{2} s_1^4 s_3^4 + \frac{\xi_1}{2} c_1^2 s_1^2 c_3^2 + \frac{\xi_2}{2} c_1^2 s_1^2 s_3^2 + \psi_3 s_1^4 c_3^2 s_3^2. \tag{2.22}$$

The oblique parameter T is given by [36]

$$T = T_{\text{singlets}} = \frac{3 s_1^2}{16 \pi s_w^2 m_W^2} \left\{ F\left(M_1, m_W^2\right) - F\left(M_1, m_Z^2\right) \right. \tag{2.23a}$$

$$- c_2^2 \left[F\left(M_2, m_W^2\right) - F\left(M_2, m_Z^2\right) \right] \tag{2.23b}$$

$$\left. - s_2^2 \left[F\left(M_3, m_W^2\right) - F\left(M_3, m_Z^2\right) \right] \right\}, \tag{2.23c}$$

where

$$F\left(x, y\right) = \begin{cases} \dfrac{x+y}{2} - \dfrac{xy}{x-y} \ln \dfrac{x}{y} & \Leftarrow x \neq y, \\ 0 & \Leftarrow x = y. \end{cases} \tag{2.24}$$

In our numerical work we use as input the nine quantities v, w_1, w_2, M_1, M_2, M_3, ϑ_1, ϑ_2, and ϑ_3, which are equivalent to the nine parameters of the scalar potential μ_1, m_1^2, m_2^2, λ_1, ψ_1, ψ_2, ψ_3, ξ_1, and ξ_2. We input equations (1.6) and choose arbitrary values for $M_2 > 0$ and $M_3 > 0$ such that $M_2 \leq M_3$ (this represents no lack of generality, it is just the naming convention for h_2 and h_3). We enforce no lower bound on M_2 and M_3, in particular we allow them to be lower than $M_1 = (125\,\text{GeV})^2$. The VEVs w_1 and w_2 are chosen positive; this corresponds to the freedom of choice of the signs of S_1 and S_2. The angle ϑ_1 is in either the first or the fourth quadrant, with

$$\cos \vartheta_1 > 0.9, \tag{2.25}$$

so that the $h_1 W^+ W^-$ coupling is within 10% of its Standard Model value. The angle ϑ_2 is in the first quadrant; this corresponds to a choice of the signs of the fields h_2 and h_3. The angle ϑ_3 may be in any quadrant. We firstly compute T according to equation (2.23) and check
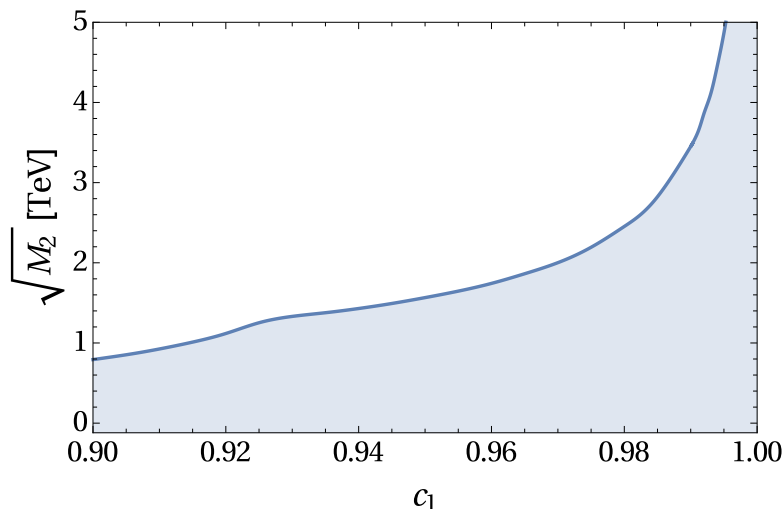
Figure 1. The upper bound on the mass of the second-lightest scalar $\sqrt{M_2}$ *versus* $\cos\vartheta_1$ in the SM2S.

that it is inside its experimentally allowed domain [4] $-0.04 < T < 0.20$. We then compute

$$\lambda_1 = \frac{1}{2v^2}\left(M_1 c_1^2 + M_2 s_1^2 c_2^2 + M_3 s_1^2 s_2^2\right), \tag{2.26a}$$

$$\psi_1 = \frac{1}{4w_1^2}\left[M_1 s_1^2 c_3^2 + M_2\left(c_1 c_2 c_3 + s_2 s_3\right)^2 + M_3\left(c_1 s_2 c_3 - c_2 s_3\right)^2\right], \tag{2.26b}$$

$$\psi_2 = \frac{1}{4w_2^2}\left[M_1 s_1^2 s_3^2 + M_2\left(c_1 c_2 s_3 - s_2 c_3\right)^2 + M_3\left(c_1 s_2 s_3 + c_2 c_3\right)^2\right], \tag{2.26c}$$

$$\xi_1 = \frac{1}{2\sqrt{2}vw_1}\left[M_1 c_1 s_1 c_3 - M_2 c_1 s_1 c_2^2 c_3 - M_3 c_1 s_1 s_2^2 c_3\right.$$
$$\left.+ (M_3 - M_2)\, s_1 c_2 s_2 s_3\right], \tag{2.26d}$$

$$\xi_2 = \frac{1}{2\sqrt{2}vw_2}\left[M_1 c_1 s_1 s_3 - M_2 c_1 s_1 c_2^2 s_3 - M_3 c_1 s_1 s_2^2 s_3\right.$$
$$\left.+ (M_2 - M_3)\, s_1 c_2 s_2 c_3\right], \tag{2.26e}$$

$$\psi_3 = \frac{1}{4w_1 w_2}\left[M_1 s_1^2 c_3 s_3 + M_2\left(c_1^2 c_2^2 - s_2^2\right) c_3 s_3 + M_3\left(c_1^2 s_2^2 - c_2^2\right) c_3 s_3\right.$$
$$\left.+ (M_3 - M_2)\, c_1 c_2 s_2\left(c_3^2 - s_3^2\right)\right]. \tag{2.26f}$$

We validate the input if the inequalities (2.8), (2.12), and (2.13) hold and if the moduli of all three eigenvalues of the matrix (2.9) are smaller than 4π.

2.4 Results

A remarkable result of our numerical work is that there is an upper bound on the mass $\sqrt{M_2}$; even if the VEVs w_1 and w_2 are allowed to be as high as $100\,\mathrm{TeV}$ — and, correspondingly, the mass $\sqrt{M_3}$ also grows to a value of that order — the mass $\sqrt{M_2}$ remains much smaller. In figure 1 we depict the upper bound on $\sqrt{M_2}$ as a function of c_1; when $c_1 \to 1$ the upper bound disappears, i.e. it tends to infinity. We emphasize that the bound depicted by the
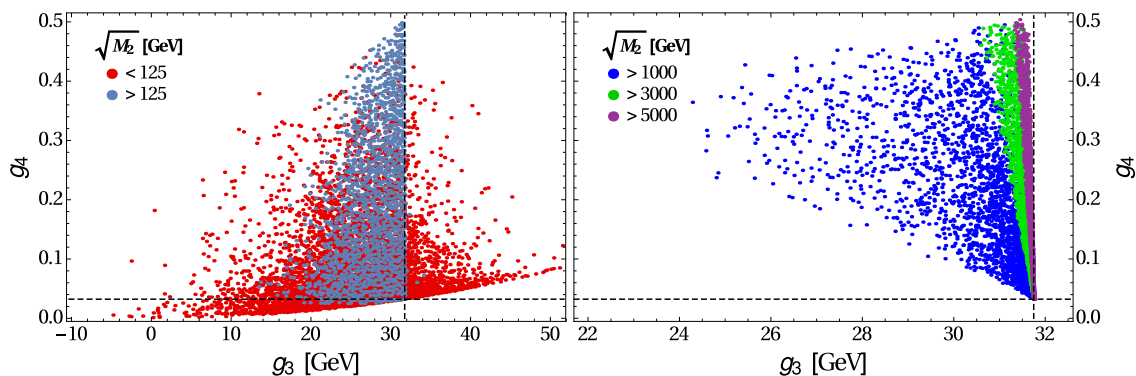
Figure 2. Scatter plots of the four-Higgs coupling g_4 *versus* the three-Higgs coupling g_3 in the SM2S. This figure was produced by randomly generating $\sqrt{M_2}$, $\sqrt{M_3}$, w_1, $w_2 \in [0\,\text{TeV}, 10\,\text{TeV}]$. The dashed lines mark the values of g_3 and g_4 in the SM. The left panel includes both red points with $M_2 < M_1$ and grey points with $M_2 > M_1$; the right panel depicts points that have $\sqrt{M_2}$ larger than either 1, 3, or 5 TeV. (In order not to overcrowd the left panel, we have used in it just a subset of the set of large-M_2 points that we have generated.)
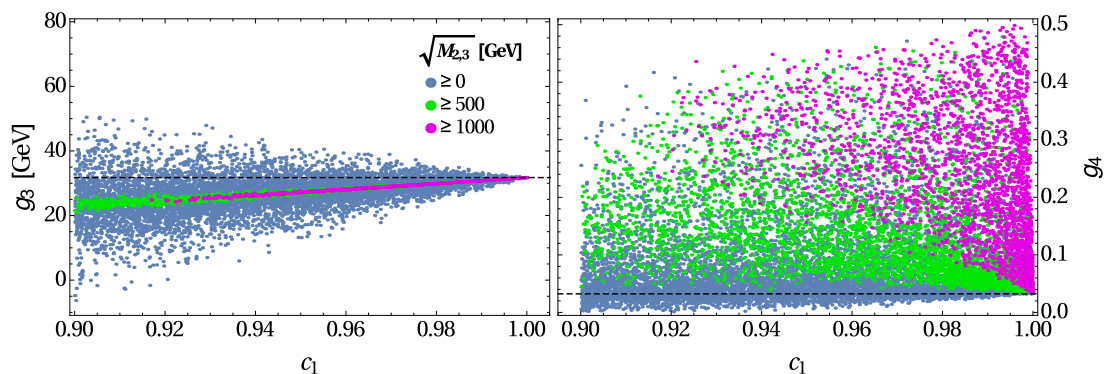

Figure 3. Scatter plots of the three-Higgs coupling g_3 (left panel) and of the four-Higgs coupling g_4 (right panel) *versus* $\cos\vartheta_1$ in the SM2S. The dashed lines mark the values of the couplings in the SM.

solid line in figure 1 was obtained through a random scan of the parameter space; it is not an analytical bound.

In figure 2 we display the predictions for g_3 and g_4. In order to produce that figure we have randomly generated $\sqrt{M_2}$, $\sqrt{M_3}$, and the VEVs w_1 and w_2 in the range 0 to 10 TeV. One sees that g_3 is always positive but below its SM value when $M_2 > M_1$; when $M_2 < M_1$ the allowed range for g_3 becomes much wider. When the masses of the new scalars get higher, g_3 takes values closer to the SM value. An important point is that g_3 remains of the same order of magnitude as in the SM, but g_4 may reach 15 times its SM value.

In the left panel of figure 3 one sees that when $\cos\vartheta_1 \to 1$ the coupling g_3 necessarily approaches its SM value. This behaviour is because of equation (2.21e) and $c_1 > 0.9$, which implies $|s_1| \ll c_1$. On the other hand, g_4 is not correlated with $\cos\vartheta_1$, as one sees in the right panel of figure 3.

3 The two-Higgs-doublet model

We next consider the model with two scalar gauge-SU(2) doublets ϕ_1 and ϕ_2 having the same weak hypercharge. This is usually known as 2HDM. The scalar potential is given by equation (2.1a), where

$$V_2 = \mu_1 \phi_1^\dagger \phi_1 + \mu_2 \phi_2^\dagger \phi_2 + \left(\mu_3 \phi_1^\dagger \phi_2 + \text{H.c.} \right), \tag{3.1a}$$

$$V_4 = \frac{\lambda_1}{2} \left(\phi_1^\dagger \phi_1 \right)^2 + \frac{\lambda_2}{2} \left(\phi_2^\dagger \phi_2 \right)^2 + \lambda_3 \, \phi_1^\dagger \phi_1 \, \phi_2^\dagger \phi_2 + \lambda_4 \, \phi_1^\dagger \phi_2 \, \phi_2^\dagger \phi_1 \tag{3.1b}$$

$$+ \left[\frac{\lambda_5}{2} \left(\phi_1^\dagger \phi_2 \right)^2 + \lambda_6 \, \phi_1^\dagger \phi_1 \, \phi_1^\dagger \phi_2 + \lambda_7 \, \phi_2^\dagger \phi_2 \, \phi_1^\dagger \phi_2 + \text{H.c.} \right], \tag{3.1c}$$

where $\mu_{1,2}$ and $\lambda_{1,2,3,4}$ are real. The ten (real) coefficients in V_4 may be grouped as [37]

$$\eta_{00} = \lambda_1 + \lambda_2 + 2\lambda_3, \tag{3.2a}$$

$$\eta = \begin{pmatrix} \eta_1 \\ \eta_2 \\ \eta_3 \end{pmatrix} = \begin{pmatrix} 2\,\Re(\lambda_6 + \lambda_7) \\ -2\,\Im(\lambda_6 + \lambda_7) \\ \lambda_1 - \lambda_2 \end{pmatrix}, \tag{3.2b}$$

$$E = \begin{pmatrix} \eta_{11} & \eta_{12} & \eta_{13} \\ \eta_{12} & \eta_{22} & \eta_{23} \\ \eta_{13} & \eta_{23} & \eta_{33} \end{pmatrix} = \begin{pmatrix} 2\lambda_4 + 2\,\Re\lambda_5 & -2\,\Im\lambda_5 & 2\,\Re(\lambda_6 - \lambda_7) \\ -2\,\Im\lambda_5 & 2\lambda_4 - 2\,\Re\lambda_5 & -2\,\Im(\lambda_6 - \lambda_7) \\ 2\,\Re(\lambda_6 - \lambda_7) & -2\,\Im(\lambda_6 - \lambda_7) & \lambda_1 + \lambda_2 - 2\lambda_3 \end{pmatrix}. \tag{3.2c}$$

Under a (unitary) change of basis of the scalar doublets, η_{00} is invariant while

$$\eta \to O\eta, \quad E \to OEO^T, \tag{3.3}$$

where O is an SO(3) matrix. Only quantities and procedures that are invariant under the transformation (3.3) are meaningful.

3.1 Unitarity conditions

We write

$$\phi_1 = \begin{pmatrix} a \\ b \end{pmatrix}, \quad \phi_2 = \begin{pmatrix} c \\ d \end{pmatrix}, \quad \phi_1^\dagger = \begin{pmatrix} a^* & b^* \end{pmatrix}, \quad \phi_2^\dagger = \begin{pmatrix} c^* & d^* \end{pmatrix}. \tag{3.4}$$

– 11 –

Then,

$$V_4 = \lambda_1 \left(\frac{a^*a^*aa + b^*b^*bb}{2} + a^*b^*ab \right) \tag{3.5a}$$

$$+ \lambda_2 \left(\frac{c^*c^*cc + d^*d^*dd}{2} + c^*d^*cd \right) \tag{3.5b}$$

$$+ (\lambda_3 + \lambda_4)\,(a^*c^*ac + b^*d^*bd) \tag{3.5c}$$

$$+ \lambda_3\,(a^*d^*ad + b^*c^*bc) \tag{3.5d}$$

$$+ \lambda_4\,(a^*d^*bc + b^*c^*ad) \tag{3.5e}$$

$$+ \lambda_5 \left(\frac{a^*a^*cc + b^*b^*dd}{2} + a^*b^*cd \right) \tag{3.5f}$$

$$+ \lambda_5^* \left(\frac{c^*c^*aa + d^*d^*bb}{2} + c^*d^*ab \right) \tag{3.5g}$$

$$+ \lambda_6\,(a^*a^*ac + b^*b^*bd + a^*b^*ad + a^*b^*bc) \tag{3.5h}$$

$$+ \lambda_6^*\,(a^*c^*aa + b^*d^*bb + a^*d^*ab + b^*c^*ab) \tag{3.5i}$$

$$+ \lambda_7\,(a^*c^*cc + b^*d^*dd + b^*c^*cd + a^*d^*cd) \tag{3.5j}$$

$$+ \lambda_7^*\,(c^*c^*ac + d^*d^*bd + c^*d^*bc + c^*d^*ad)\,. \tag{3.5k}$$

The relevant scattering channels are [33]:

1. The channel $Q = 2$, $T_3 = 1$, with three states aa, cc, and ac.

2. The channel $Q = 0$, $T_3 = -1$, with three states bb, dd, and bd.

3. The channel $Q = 1$, $T_3 = 0$, with four states ab, cd, ad, and bc.

4. The channel $Q = 1$, $T_3 = 1$, with four states ab^*, cd^*, ad^*, and cb^*.

5. The channel $Q = 0$, $T_3 = 0$, with eight states aa^*, bb^*, cc^*, dd^*, ac^*, bd^*, ca^*, and db^*.

Channel 5 produces the scattering matrix

$$\begin{pmatrix}
2\lambda_1 & \lambda_1 & \lambda_3 + \lambda_4 & \lambda_3 & 2\lambda_6^* & \lambda_6^* & 2\lambda_6 & \lambda_6 \\
\lambda_1 & 2\lambda_1 & \lambda_3 & \lambda_3 + \lambda_4 & \lambda_6^* & 2\lambda_6^* & \lambda_6 & 2\lambda_6 \\
\lambda_3 + \lambda_4 & \lambda_3 & 2\lambda_2 & \lambda_2 & 2\lambda_7^* & \lambda_7^* & 2\lambda_7 & \lambda_7 \\
\lambda_3 & \lambda_3 + \lambda_4 & \lambda_2 & 2\lambda_2 & \lambda_7^* & 2\lambda_7^* & \lambda_7 & 2\lambda_7 \\
2\lambda_6 & \lambda_6 & 2\lambda_7 & \lambda_7 & \lambda_3 + \lambda_4 & \lambda_4 & 2\lambda_5 & \lambda_5 \\
\lambda_6 & 2\lambda_6 & \lambda_7 & 2\lambda_7 & \lambda_4 & \lambda_3 + \lambda_4 & \lambda_5 & 2\lambda_5 \\
2\lambda_6^* & \lambda_6^* & 2\lambda_7^* & \lambda_7^* & 2\lambda_5^* & \lambda_5^* & \lambda_3 + \lambda_4 & \lambda_4 \\
\lambda_6^* & 2\lambda_6^* & \lambda_7^* & 2\lambda_7^* & \lambda_5^* & 2\lambda_5^* & \lambda_4 & \lambda_3 + \lambda_4
\end{pmatrix}. \tag{3.6}$$

A similarity transformation transforms the matrix (3.6) into the direct sum of two 4×4 matrices

$$\mathcal{M}_1 = \frac{1}{2} \begin{pmatrix} \eta_{00} - 2I & \eta^T \\ \eta & E + 2I \times \mathbb{1}_{3\times3} \end{pmatrix}, \tag{3.7a}$$

$$\mathcal{M}_2 = \frac{1}{2} \begin{pmatrix} 3\eta_{00} - 2I & 3\eta^T \\ 3\eta & 3E + 2I \times \mathbb{1}_{3\times3} \end{pmatrix}. \tag{3.7b}$$

Here,

$$I = \lambda_3 - \lambda_4 = \frac{\eta_{00} - \operatorname{tr} E}{4} \qquad (3.8)$$

is invariant under a change of basis of the doublets. It is obvious that the eigenvalues of the matrices (3.7) are invariant under such a change too.

Channel 4 produces the scattering matrix

$$\begin{pmatrix} \lambda_1 & \lambda_4 & \lambda_6^* & \lambda_6 \\ \lambda_4 & \lambda_2 & \lambda_7^* & \lambda_7 \\ \lambda_6 & \lambda_7 & \lambda_3 & \lambda_5 \\ \lambda_6^* & \lambda_7^* & \lambda_5^* & \lambda_3 \end{pmatrix}, \qquad (3.9)$$

which may readily be shown to be similar to $\mathcal{M}_1$. Channel 3 produces the scattering matrix

$$\begin{pmatrix} \lambda_1 & \lambda_5 & \lambda_6 & \lambda_6 \\ \lambda_5^* & \lambda_2 & \lambda_7^* & \lambda_7^* \\ \lambda_6^* & \lambda_7 & \lambda_3 & \lambda_4 \\ \lambda_6^* & \lambda_7 & \lambda_4 & \lambda_3 \end{pmatrix}. \qquad (3.10)$$

The matrix (3.10) is similar to

$$\begin{pmatrix} & & & 0 \\ & \mathcal{M}_3 & & 0 \\ & & & 0 \\ 0 & 0 & 0 & I \end{pmatrix}, \qquad (3.11)$$

where

$$\mathcal{M}_3 = \begin{pmatrix} \lambda_1 & \lambda_5 & \sqrt{2}\lambda_6 \\ \lambda_5^* & \lambda_2 & \sqrt{2}\lambda_7^* \\ \sqrt{2}\lambda_6^* & \sqrt{2}\lambda_7 & \lambda_3 + \lambda_4 \end{pmatrix}. \qquad (3.12)$$

Channels 1 and 2 also lead to the matrix $\mathcal{M}_3$. Direct computation demonstrates that the eigenvalues of $\mathcal{M}_3$ are invariant under the transformation (3.3).

Thus, the unitarity conditions for the scalar potential of the 2HDM are the following: the eigenvalues of the two 4×4 matrices (3.7) and of the 3×3 matrix (3.12), and I in equation (3.8), should have moduli smaller than 4π. These conditions were first derived in refs. [38, 39]. We emphasize that they are, as they should, invariant under a change of basis of the two doublets.

3.1.1 The case $\lambda_6 = \lambda_7 = 0$

If $\lambda_6 = \lambda_7 = 0$, then $\eta_1 = \eta_2 = \eta_{13} = \eta_{23} = 0$ and this simplifies things considerably. The unitarity conditions are then

$$|\lambda_3 + \lambda_4| < 4\pi, \tag{3.13a}$$

$$|\lambda_3 - \lambda_4| < 4\pi, \tag{3.13b}$$

$$|\lambda_3 + |\lambda_5|| < 4\pi, \tag{3.13c}$$

$$|\lambda_3 - |\lambda_5|| < 4\pi, \tag{3.13d}$$

$$a_+ \equiv |\lambda_3 + 2\lambda_4 + 3|\lambda_5|| < 4\pi, \tag{3.13e}$$

$$a_- \equiv |\lambda_3 + 2\lambda_4 - 3|\lambda_5|| < 4\pi, \tag{3.13f}$$

$$\left|\lambda_1 + \lambda_2 + \sqrt{(\lambda_1 - \lambda_2)^2 + 4|\lambda_5|^2}\right| < 8\pi, \tag{3.13g}$$

$$\left|\lambda_1 + \lambda_2 - \sqrt{(\lambda_1 - \lambda_2)^2 + 4|\lambda_5|^2}\right| < 8\pi, \tag{3.13h}$$

$$\left|\lambda_1 + \lambda_2 + \sqrt{(\lambda_1 - \lambda_2)^2 + 4\lambda_4^2}\right| < 8\pi, \tag{3.13i}$$

$$\left|\lambda_1 + \lambda_2 - \sqrt{(\lambda_1 - \lambda_2)^2 + 4\lambda_4^2}\right| < 8\pi, \tag{3.13j}$$

$$b_+ \equiv \left|3\lambda_1 + 3\lambda_2 + \sqrt{9(\lambda_1 - \lambda_2)^2 + 4(2\lambda_3 + \lambda_4)^2}\right| < 8\pi, \tag{3.13k}$$

$$b_- \equiv \left|3\lambda_1 + 3\lambda_2 - \sqrt{9(\lambda_1 - \lambda_2)^2 + 4(2\lambda_3 + \lambda_4)^2}\right| < 8\pi. \tag{3.13l}$$

3.1.2 The case $\lambda_1 = \lambda_2 = \lambda_3 = \lambda_4 = \lambda_5 = 0$

The case $\lambda_1 = \lambda_2 = \lambda_3 = \lambda_4 = \lambda_5 = 0$ is not realistic because it produces a potential unbounded from below. Still, one may compute the unitarity conditions in that case and one obtains

$$\sqrt{|\lambda_6|^2 + |\lambda_7|^2} < 2\sqrt{2}\pi, \tag{3.14a}$$

$$\sqrt{|\lambda_6|^2 + |\lambda_7|^2 + |\lambda_6^2 + \lambda_7^2|} < \frac{4\pi}{3}. \tag{3.14b}$$

3.1.3 Consequences

We have numerically analyzed the unitarity conditions by giving random values to λ_1, λ_2, λ_3, λ_4, $|\lambda_5|$, $|\lambda_6|$, $|\lambda_7|$, $\arg(\lambda_5^* \lambda_6 \lambda_7)$, and $\arg(\lambda_6^* \lambda_7)$ and then checking whether all the unitarity conditions are met. We present in figures 4–6 scatter plots with more than 8,000 allowed points each. We have found that all the conditions (3.13) still hold even when $\lambda_6 = \lambda_7 = 0$ is not true; also, the conditions (3.14) still hold even when $\lambda_1 = \lambda_2 = \lambda_3 = \lambda_4 = \lambda_5 = 0$ does not apply. In particular, the upper bounds (3.13b), (3.13e), (3.13f), (3.13k), and (3.13l) are sometimes attained, as illustrated in figures 6 and 5, respectively. For the
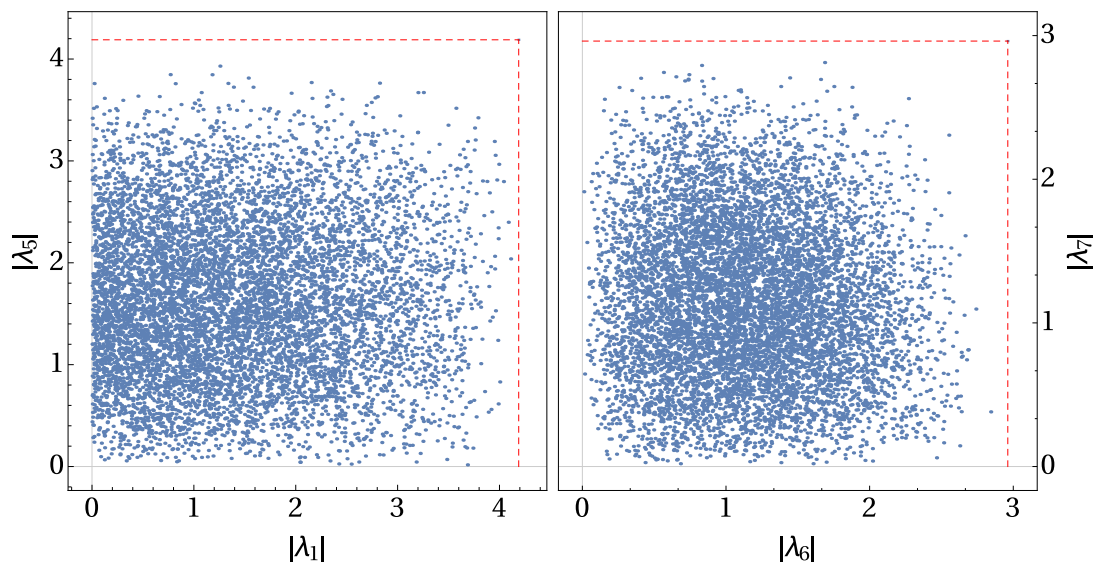
Figure 4. Scatter plots of $|\lambda_1|$ *versus* $|\lambda_5|$ and of $|\lambda_6|$ *versus* $|\lambda_7|$ with the unitarity conditions enforced. The dashed red lines indicate the bounds $|\lambda_{1,5}| < 4\pi/3$ and $|\lambda_{6,7}| < 2\sqrt{2}\pi/3$, respectively.
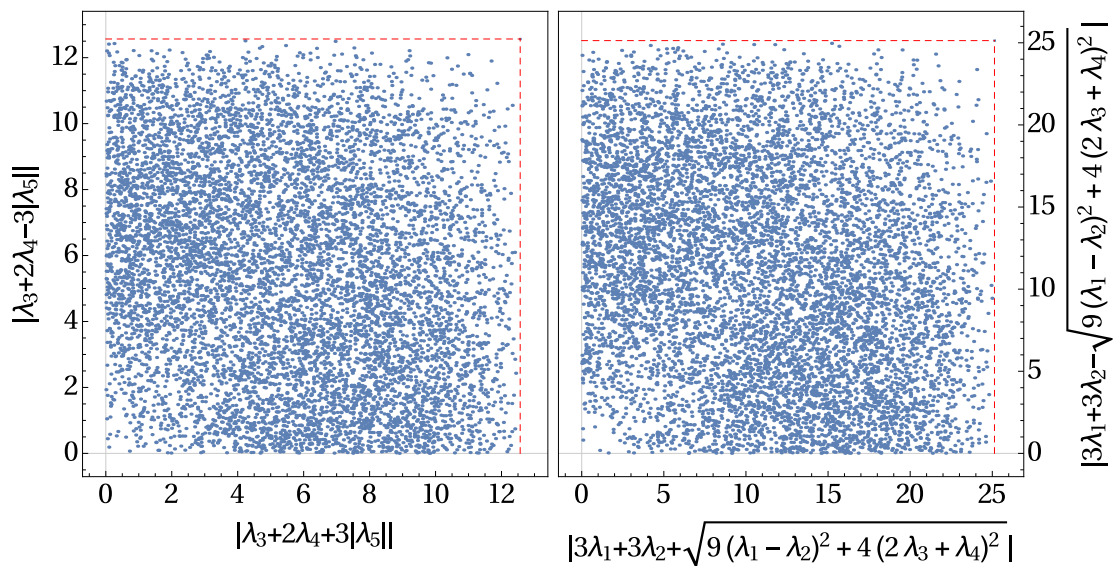

Figure 5. Scatter plots of $a_\pm$ and $b_\pm$ — see equations (3.13e), (3.13f), (3.13k), and (3.13l) — with the unitarity conditions enforced. The red dashed lines indicate the bounds $a_\pm < 4\pi$ in the left plot and $b_\pm < 8\pi$ in the right plot.
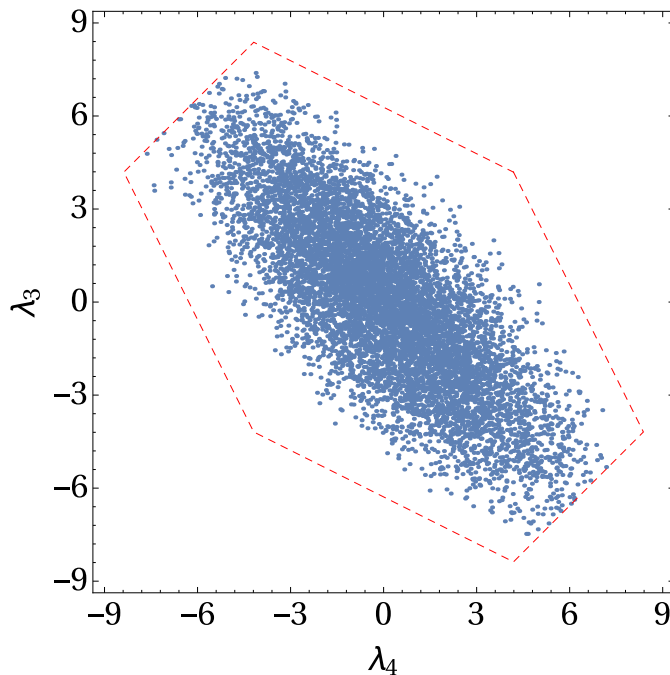
Figure 6. Scatter plots of λ_3 *versus* λ_4 with the unitarity conditions enforced. The dashed red lines are given by the equations $|\lambda_3 - \lambda_4| = 4\pi$, $|2\lambda_3 + \lambda_4| = 4\pi$, and $|\lambda_3 + 2\lambda_4| = 4\pi$.

individual parameters, the bounds

$$|\lambda_{1,2}| < \frac{4\pi}{3}, \tag{3.15a}$$

$$|\lambda_5| < \frac{4\pi}{3}, \tag{3.15b}$$

$$|\lambda_{6,7}| < \frac{2\sqrt{2}\pi}{3} \tag{3.15c}$$

hold and are illustrated in figure 4; the bound (3.15a) is suggested by inequality (3.13k) when λ_3, λ_4, and either λ_1 or λ_2 vanish; the bound (3.15b) is suggested by inequality (3.13e) when $\lambda_3 = \lambda_4 = 0$, and the bound (3.15c) is suggested by inequality (3.14b) when either λ_6 or λ_7 vanishes. Finally, (λ_3, λ_4) is always within the hexagon with sides $|\lambda_3 - \lambda_4| = 4\pi$, $|2\lambda_3 + \lambda_4| = 4\pi$, and $|\lambda_3 + 2\lambda_4| = 4\pi$, as illustrated in figure 6.

3.2 Bounded-from-below conditions

Necessary and sufficient conditions for the scalar potential of the 2HDM to be BFB were first derived in ref. [37]. Ivanov [40] and Silva [41] later produced other, equivalent conditions to the same effect. We have implemented numerically both the conditions of ref. [37] and those of ref. [41]. We have found that the Ivanov-Silva algorithm runs several times faster than the one of ref. [37]. We have also checked that all the points produced by either algorithm were validated by the other one.

The points in our scatter plots were produced by using the algorithm of ref. [41]. That algorithm runs as follows. One constructs the 4×4 matrix

$$\Lambda_E = \begin{pmatrix} \eta_{00} & \eta^T \\ -\eta & -E \end{pmatrix} \tag{3.16}$$

and one computes its four eigenvalues. Then the potential is BFB if all the following conditions apply:

- All four eigenvalues are real.

- All four eigenvalues are different from each other.

- Call Λ_0 the largest eigenvalue. Call the other three eigenvalues $\Lambda_{1,2,3}$. The eigenvalue Λ_0 is positive; thus,

$$\Lambda_0 > \Lambda_{1,2,3}, \quad \Lambda_0 > 0. \tag{3.17}$$

(Each of Λ_1, Λ_2, and Λ_3 may be either positive or negative.)

-
$$\frac{[(\Lambda_E - \Lambda_1 \times \mathbb{1}_{4\times4}) \times (\Lambda_E - \Lambda_2 \times \mathbb{1}_{4\times4}) \times (\Lambda_E - \Lambda_3 \times \mathbb{1}_{4\times4})]_{11}}{(\Lambda_0 - \Lambda_1)(\Lambda_0 - \Lambda_2)(\Lambda_0 - \Lambda_3)} > 0. \tag{3.18}$$

It is possible to derive analytically some necessary conditions for boundedness-from-below. Let us parameterize

$$\phi_1^\dagger \phi_1 = r^2 \sin^2 \theta, \quad \phi_2^\dagger \phi_2 = r^2 \cos^2 \theta, \quad \phi_1^\dagger \phi_2 = e^{i\alpha} r^2 h \sin \theta \cos \theta, \tag{3.19}$$

where $0 \le \theta \le \pi/2$ without loss of generality. Since, in the notation of equations (3.4),

$$r^4 \left(1 - h^2\right) \sin^2 \theta \cos^2 \theta = \phi_1^\dagger \phi_1 \, \phi_2^\dagger \phi_2 - \phi_1^\dagger \phi_2 \, \phi_2^\dagger \phi_1 = |ad - bc|^2 \ge 0, \tag{3.20}$$

one concludes that $h^2 \le 1$. Thus, without loss of generality $0 \le h \le 1$ while the phase α is arbitrary. Boundedness from below of V_4 means that

$$\frac{\lambda_1}{2} \sin^4 \theta + \frac{\lambda_2}{2} \cos^4 \theta + \left[\lambda_3 + \lambda_4 h^2 + \Re\!\left(\lambda_5 e^{2i\alpha}\right) h^2\right] \sin^2 \theta \cos^2 \theta \tag{3.21a}$$

$$+ 2h \, \Re\!\left(\lambda_6 e^{i\alpha}\right) \sin^3 \theta \cos \theta + 2h \, \Re\!\left(\lambda_7 e^{i\alpha}\right) \sin \theta \cos^3 \theta > 0 \tag{3.21b}$$

for any θ, h, and α. From the cases $\theta = 0$ and $\theta = \pi/2$ one derives

$$\lambda_1 > 0, \quad \lambda_2 > 0. \tag{3.22}$$

Making $\alpha \to \pi + \alpha$ in inequality (3.21), one concludes that

$$2h \sin \theta \cos \theta \left|\Re\!\left[\left(\lambda_6 \sin^2 \theta + \lambda_7 \cos^2 \theta\right) e^{i\alpha}\right]\right| < \frac{\lambda_1}{2} \sin^4 \theta + \frac{\lambda_2}{2} \cos^4 \theta \tag{3.23a}$$

$$+ \left[\lambda_3 + \lambda_4 h^2\right. \tag{3.23b}$$

$$\left. + \Re\!\left(\lambda_5 e^{2i\alpha}\right) h^2\right] \sin^2 \theta \cos^2 \theta. \tag{3.23c}$$

Therefore, the quantity in the right-hand side of inequality (3.23) must be positive for any θ, h, and α. It is easy to see that

$$\varrho \sin^4 \theta + \varsigma \cos^4 \theta + \varepsilon \sin^2 \theta \cos^2 \theta > 0 \ \ \forall \theta \in \left[0, \ \frac{\pi}{2}\right] \Leftrightarrow \varrho > 0, \ \varsigma > 0, \ \varepsilon > -2\sqrt{\varrho\varsigma}. \quad (3.24)$$

Applying the statement (3.24) to the case $\varrho = \lambda_1/2$, $\varsigma = \lambda_2/2$, $\varepsilon = \lambda_3 + \lambda_4 h^2 + \Re\left(\lambda_5 e^{2i\alpha}\right)h^2$ for any $h \in [0, \ 1]$ and α, one concludes that

$$\lambda_3 > -\sqrt{\lambda_1 \lambda_2}, \quad \lambda_3 + \lambda_4 - |\lambda_5| > -\sqrt{\lambda_1 \lambda_2}. \quad (3.25)$$

Inequalities (3.22) and (3.25) are necessary and sufficient conditions for boundedness-from-below when $\lambda_6 = \lambda_7 = 0$ [42, 43]; they are necessary conditions when λ_6 and λ_7 are nonzero.

We may now return to inequality (3.23), which implies, in principle, many more necessary conditions for boundedness-from-below. Setting for instance $\sin\theta = \cos\theta$ one concludes that

$$2h \left|\Re\left[(\lambda_6 + \lambda_7) e^{i\alpha}\right]\right| < \frac{\lambda_1 + \lambda_2}{2} + \lambda_3 + \lambda_4 h^2 + \Re\left(\lambda_5 e^{2i\alpha}\right)h^2, \quad (3.26)$$

which must hold for any h and α. Therefore [44],

$$2\left|\lambda_6 + \lambda_7\right| < \frac{\lambda_1 + \lambda_2}{2} + \lambda_3 + \lambda_4 + |\lambda_5|. \quad (3.27)$$

We have numerically analyzed the BFB conditions by giving random values to λ_1, λ_2, λ_3, λ_4, $|\lambda_5|$, $|\lambda_6|$, $|\lambda_7|$, $\arg\left(\lambda_5^* \lambda_6 \lambda_7\right)$, and $\arg\left(\lambda_6^* \lambda_7\right)$ and then checking whether the BFB conditions are met. We have confirmed that the conditions (3.22), (3.25), and (3.27) always hold.[6]

3.3 Procedure

We consider the most general 2HDM and purport to find out its ranges for g_3 and g_4. We use the Higgs basis for the scalar doublets; in that basis only ϕ_1^0 has VEV and therefore ϕ_1 has the expression (1.2), while

$$\phi_2 = \begin{pmatrix} C^+ \\ \left(\sigma_1 + i\sigma_2\right)/\sqrt{2} \end{pmatrix}. \quad (3.28)$$

In equation (3.28), σ_1 and σ_2 are real fields and C^+ is the physical charged scalar of the 2HDM. We emphasize that using the Higgs basis represents no lack of generality, because both the unitarity and the BFB conditions are the same in any basis.

Since only ϕ_1 has VEV, the vacuum stability conditions are $\mu_1 = -\lambda_1 v^2$ and $\mu_3 = -\lambda_6 v^2$ [46]. The coupling μ_2 in equation (3.1a) is unrelated to the parameters of V_4; one may trade it for the charged-Higgs squared mass $M_C = \mu_2 + \lambda_3 v^2$. The mass terms of H, σ_1, and σ_2 are given by line (2.15b), with [46]

$$M = \begin{pmatrix} 2\lambda_1 v^2 & 2v^2 \Re\lambda_6 & -2v^2 \Im\lambda_6 \\ 2v^2 \Re\lambda_6 & M_C + (\lambda_4 + \Re\lambda_5) v^2 & -v^2 \Im\lambda_5 \\ -2v^2 \Im\lambda_6 & -v^2 \Im\lambda_5 & M_C + (\lambda_4 - \Re\lambda_5) v^2 \end{pmatrix}. \quad (3.29)$$

The matrix M is diagonalized through equations (2.17)–(2.19).

---

[6]The BFB conditions worked out in this subsection are, clearly, the ones valid at tree level. At loop level the BFB conditions change, see ref. [45].

The three invariants of M are

$$I_1(M) = 2M_C + 2\left(\lambda_1 + \lambda_4\right)v^2, \tag{3.30a}$$

$$I_2(M) = M_C^2 + 2\left(2\lambda_1 + \lambda_4\right)v^2 M_C + \left(4\lambda_1\lambda_4 + \lambda_4^2 - |\lambda_5|^2 - 4|\lambda_6|^2\right)v^4, \tag{3.30b}$$

$$I_3(M) = 2\lambda_1 v^2 M_C^2 + 4\left(\lambda_1\lambda_4 - |\lambda_6|^2\right)v^4 M_C$$
$$+ 2\left[\lambda_1\lambda_4^2 - \lambda_1|\lambda_5|^2 - 2\lambda_4|\lambda_6|^2 + 2\Re\left(\lambda_5^*\lambda_6^2\right)\right]v^6. \tag{3.30c}$$

We input parameters $\lambda_{1,2,\cdots,7}$ that satisfy both the unitarity conditions and the BFB conditions of subsections 3.1 and 3.2, respectively.[7] We also use the values of M_1 and v in equations (1.6). The two equations

$$M_1^3 - M_1^2 I_1(M) + M_1 I_2(M) - I_3(M) = 0, \tag{3.31a}$$

$$\left[M_1^2 I_1(M) - 2M_1 I_2(M) + 3I_3(M)\right]\cos^2\vartheta_1$$
$$+ M_{11}\left[M_1 I_1(M) - M_1^2\right] - \left(M^2\right)_{11}M_1 - I_3(M) = 0 \tag{3.31b}$$

are quadratic in M_C. By affirming the fact that both quadratic equations (3.31) must hold for the same value of M_C, one is able to compute both M_C and $\cos^2\vartheta_1$. We thus get to know the full matrix M, hence its eigenvalues M_2 and M_3 and its diagonalizing matrix R.

We require $\cos\vartheta_1 > 0.9$. We also compute the oblique parameter

$$T = \frac{1}{16\pi s_w^2 m_W^2}\left[s_1^2 F\left(M_C, M_1\right) + \left(1 - s_1^2 c_2^2\right)F\left(M_C, M_2\right) + \left(1 - s_1^2 s_2^2\right)F\left(M_C, M_3\right)\right. \tag{3.32a}$$

$$\left. - c_1^2 F\left(M_2, M_3\right) - s_1^2 c_2^2 F\left(M_1, M_3\right) - s_1^2 s_2^2 F\left(M_1, M_2\right)\right] + T_{\text{singlets}}, \tag{3.32b}$$

where T_{singlets} is given by equation (2.23). We require $-0.04 < T < 0.20$.

We have applied the method devised in ref. [41] to guarantee that our assumed vacuum state is indeed the state with the lowest possible value of the potential. The method may be described as follows. Let the matrix Λ_E in equation (3.16) have four eigenvalues $\Lambda_{0,1,2,3}$. We already know, from the BFB conditions, that those eigenvalues must be real and different from each other; let us order them as $\Lambda_0 > \Lambda_1 > \Lambda_2 > \Lambda_3$. Let the charged-Higgs squared mass be M_C; define $\zeta \equiv 2M_C/v^2$. Then, the assumed vacuum state is the global minimum of the potential if either $\zeta > \Lambda_0$, or $\Lambda_0 > \zeta > \Lambda_1$, or $\Lambda_2 > \zeta > \Lambda_3$. This test led us to discard about 10% of our previous set of points.

The four-Higgs vertex is given by

$$g_4 = \frac{\lambda_1 c_1^4}{8} + \frac{\lambda_2 s_1^4}{8} + \frac{\left(\lambda_3 + \lambda_4\right)c_1^2 s_1^2}{4} + \frac{s_1^2 c_1^2\left(c_3^2 - s_3^2\right)\Re\lambda_5}{4} - \frac{s_1^2 c_1^2 c_3 s_3 \Im\lambda_5}{2} \tag{3.33a}$$

$$+ \frac{s_1 c_1^3\left(c_3\Re\lambda_6 - s_3\Im\lambda_6\right)}{2} + \frac{s_1^3 c_1\left(c_3\Re\lambda_7 - s_3\Im\lambda_7\right)}{2}. \tag{3.33b}$$

---

[7]This method, where $\lambda_{1,2,\cdots,7}$ are used as input, tends to produce few points with either very low or very high scalar masses. Therefore we have supplemented it by another search in which we have directly used as input $M_{1,2,3,C}$.
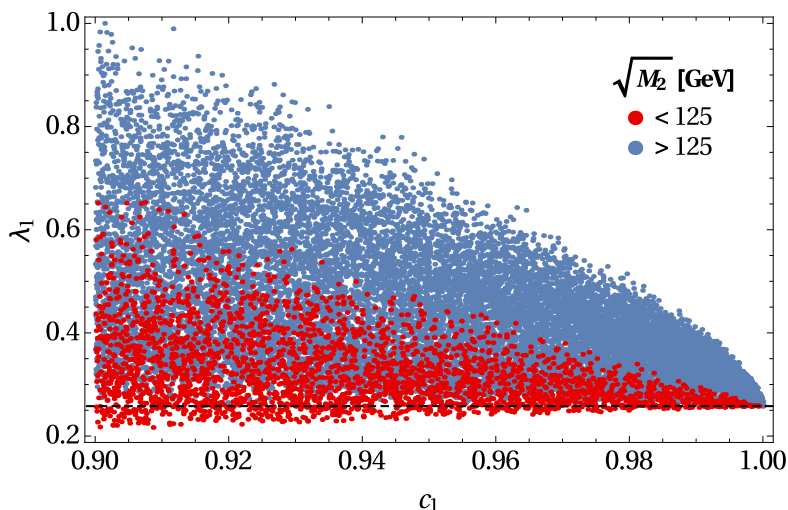
Figure 7. Scatter plots of λ_1 *versus* $\cos\vartheta_1$ in the 2HDM. The dashed line marks the value of λ_1 in the SM. The red points have $M_2 < M_1$.

The three-Higgs vertex is given by

$$g_3 = \frac{v}{\sqrt{2}} \left[\lambda_1 c_1^3 + (\lambda_3 + \lambda_4)\, s_1^2 c_1 + s_1^2 c_1 \left(c_3^2 - s_3^2 \right) \Re\lambda_5 - 2s_1^2 c_1 c_3 s_3\, \Im\lambda_5 \right. \tag{3.34a}$$

$$\left. + 3s_1 c_1^2 \left(c_3 \Re\lambda_6 - s_3 \Im\lambda_6 \right) + s_1^3 \left(c_3 \Re\lambda_7 - s_3 \Im\lambda_7 \right) \right]. \tag{3.34b}$$

We also want to consider the $h_1 C^+ C^-$ vertex, which may be relevant in the discovery of the charged scalar. That vertex is given by

$$V_4 = \cdots + h_1 C^+ C^- g_{1CC}, \tag{3.35}$$

where, in the 2HDM,

$$g_{1CC} = \sqrt{2}v \left(c_1 \lambda_3 + s_1 c_3 \Re\lambda_7 - s_1 s_3 \Im\lambda_7 \right). \tag{3.36}$$

3.4 Results

As we know from subsections 3.1 and 3.2, in general λ_1 can take any value in between 0 and $4\pi/3$. Once the constraint $\cos\vartheta_1 > 0.9$ is imposed, however, λ_1 can be no larger than ~ 1; this is illustrated in figure 7. The closer $\cos\vartheta_1$ is to 1, the closer λ_1 must be to its SM value $M_1/(2v^2) = 0.258$; note that λ_1 is almost always larger than its SM value when $\cos\vartheta_1 > 0.9$; the minimum value that we have obtained for λ_1 is 0.2135.

If $\cos\vartheta_1 \lesssim 0.99$, then the masses of the new scalar particles of the 2HDM, namely $\sqrt{M_C}$, $\sqrt{M_2}$, and $\sqrt{M_3}$ can be no larger than $\sim 700\,\text{GeV}$; if $\cos\vartheta_1 \lesssim 0.95$, they can be no larger than $\sim 550\,\text{GeV}$. When $\cos\vartheta_1$ becomes close to 1, the masses of the new scalar particles may reach O(TeV); this is illustrated in figure 8.

One sees in figure 9 that $\sqrt{M_C}$ and $\sqrt{M_2}$ differ by at most $\sim 100\,\text{GeV}$ unless $200\,\text{GeV} < \sqrt{M_C} < 500\,\text{GeV}$. (Remember that by convention M_2 is always smaller than M_3, but they may be smaller than M_1.)
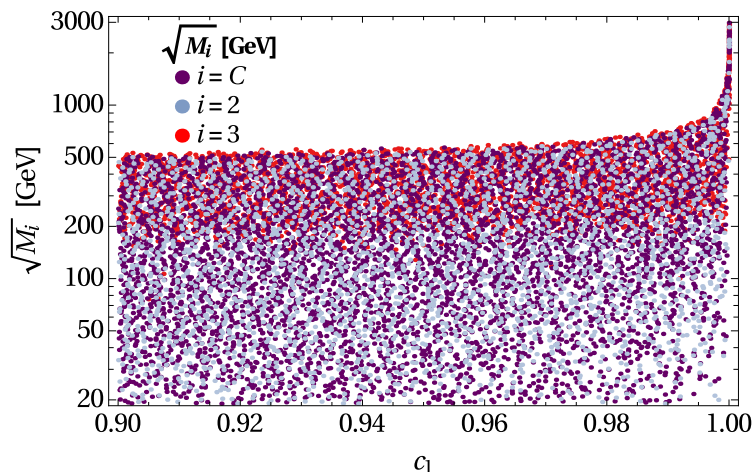
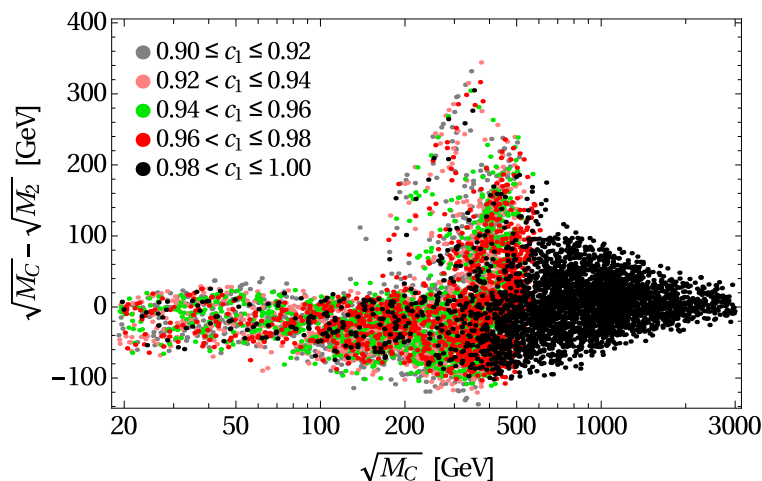**Figure 8**. Scatter plots of the masses of the extra scalars of the 2HDM *versus* $\cos\vartheta_1$.

Figure 9. The difference between the mass of the charged scalar and the mass of the lightest non-SM neutral scalar *versus* the mass of the charged scalar in the 2HDM.

We now come to the predictions for g_3 and g_4 in the 2HDM, which are depicted in figure 10. One sees that g_3 in the 2HDM has a range only slightly larger than in the SM2S, while g_4 in the 2HDM is much more restricted than in the SM2S; $g_4 / g_4^{\mathrm{SM}} \lesssim 4$ in the 2HDM but $g_4 / g_4^{\mathrm{SM}} \lesssim 15$ in the SM2S. An interesting feature is that g_3 may be zero or even negative, i.e. it may have sign opposite to the one in the SM. (We recall that the sign of g_3 is measured relative to the sign of c_1; we arrange that c_1 is always positive.) On the other hand, g_4 is always positive because of the boundedness from below of the potential.

In figure 11 we depict the coupling g_{1CC} of the 125 GeV neutral scalar to a pair of charged scalars in the 2HDM. One sees that that coupling is in between -200 GeV and 1,700 GeV. The expression for g_{1CC} in equation (3.36) is strongly dominated by the first term in the right-hand side because $c_1 \gg s_1$. The preference for positive values of g_{1CC} observed in figure 11 occurs because $-2 \lesssim \lambda_3 \lesssim 7$ in the 2HDM with the constraint $c_1 > 0.9$ enforced.
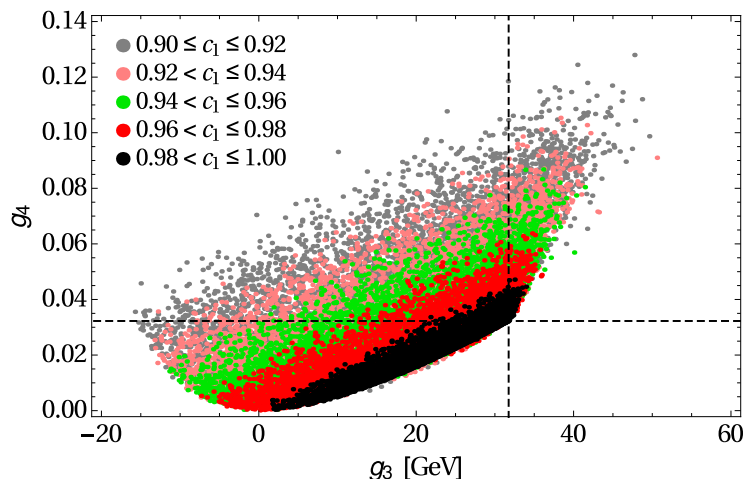
Figure 10. Scatter plot of the four-Higgs coupling g_4 *versus* the three-Higgs coupling g_3 in the 2HDM, for various values of c_1. The dashed lines mark the values of both couplings in the SM.
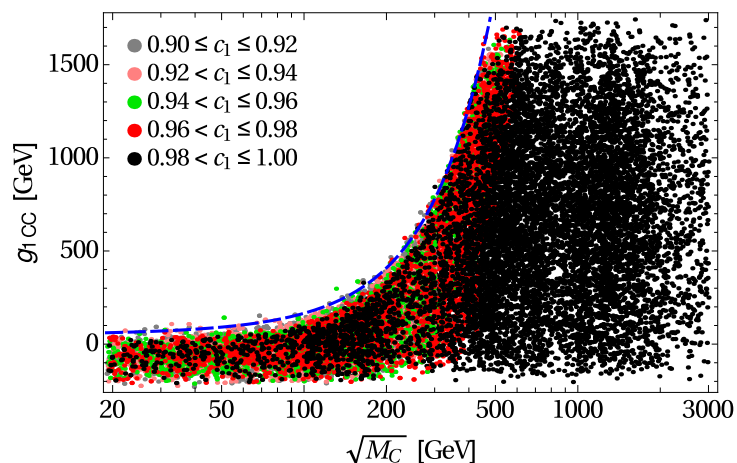

Figure 11. Scatter plot of the $h_1 C^+ C^-$ coupling g_{1CC} *versus* the mass of the charged scalars $C^\pm$ in the 2HDM. The blue line with equation $g_{1CC}/\text{GeV} = 48.5 + 0.54\left(\sqrt{M_C}/\text{GeV}\right) + 0.0063\left(M_C/\text{GeV}^2\right)$ marks the approximate boundary of the allowed region.

4   The two-Higgs-doublet model plus one singlet

We consider in this section the two-Higgs-doublet model with the addition of one real SU(2) × U(1)-invariant scalar field S. We assume a symmetry $S \to -S$. As a shorthand, we shall dub this model the 2HDM1S (other authors use just 2HDMS [47]). The quartic part of the scalar potential is

$$V_4 = \frac{\lambda_1}{2}\left(\phi_1^\dagger \phi_1\right)^2 + \frac{\lambda_2}{2}\left(\phi_2^\dagger \phi_2\right)^2 + \lambda_3\, \phi_1^\dagger \phi_1\, \phi_2^\dagger \phi_2 + \lambda_4\, \phi_1^\dagger \phi_2\, \phi_2^\dagger \phi_1 \tag{4.1a}$$

$$+ \left[\frac{\lambda_5}{2}\left(\phi_1^\dagger \phi_2\right)^2 + \lambda_6\, \phi_1^\dagger \phi_1\, \phi_1^\dagger \phi_2 + \lambda_7\, \phi_2^\dagger \phi_2\, \phi_1^\dagger \phi_2 + \text{H.c.}\right] \tag{4.1b}$$

$$+ \frac{\psi}{2}\, S^4 \tag{4.1c}$$

$$+ S^2\left(\xi_1\, \phi_1^\dagger \phi_1 + \xi_2\, \phi_2^\dagger \phi_2 + \xi_3\, \phi_1^\dagger \phi_2 + \xi_3^*\, \phi_2^\dagger \phi_1\right). \tag{4.1d}$$

4.1 Bounded-from-below conditions

Deriving necessary and sufficient BFB conditions for even a rather simple potential like the one in equation (4.1) is a notoriously difficult problem [48]. If V_4 were negative for some possible values of S^2, $\phi_1^\dagger \phi_1$, $\phi_2^\dagger \phi_2$, and $\phi_1^\dagger \phi_2$, then V_4 would tend to $-\infty$ upon multiplication of those four values by an ever-larger positive constant. Therefore, we want V_4 to be positive for all possible values of S^2, $\phi_1^\dagger \phi_1$, $\phi_2^\dagger \phi_2$, and $\phi_1^\dagger \phi_2$. In order to guarantee this, we proceed in the following fashion.

Necessary condition 1. When $S^2 = 0$, equation (4.1) reduces to its first two lines, i.e. to the quartic potential of the 2HDM. Therefore, one must require the fulfilment of the conditions of subsection 3.2, viz. the four conditions in between equations (3.16) and (3.18).

Necessary condition 2. When $\phi_1^\dagger \phi_2 = 0$,

$$V_4 = \frac{1}{2} \left(\phi_1^\dagger \phi_1 \;\; \phi_2^\dagger \phi_2 \;\; S^2 \right) \begin{pmatrix} \lambda_1 & \lambda_3 & \xi_1 \\ \lambda_3 & \lambda_2 & \xi_2 \\ \xi_1 & \xi_2 & \psi \end{pmatrix} \begin{pmatrix} \phi_1^\dagger \phi_1 \\ \phi_2^\dagger \phi_2 \\ S^2 \end{pmatrix}. \tag{4.2}$$

Since $\phi_1^\dagger \phi_1$, $\phi_2^\dagger \phi_2$, and S^2 are positive definite quantites, we must require [34, 35]

$$\psi > 0, \tag{4.3a}$$

$$\lambda_1 > 0, \tag{4.3b}$$

$$\lambda_2 > 0, \tag{4.3c}$$

$$A_1 \equiv \xi_1 + \sqrt{\lambda_1 \psi} > 0, \tag{4.3d}$$

$$A_2 \equiv \xi_2 + \sqrt{\lambda_2 \psi} > 0, \tag{4.3e}$$

$$A_3 \equiv \lambda_3 + \sqrt{\lambda_1 \lambda_2} > 0, \tag{4.3f}$$

$$\sqrt{\lambda_1 \lambda_2 \psi} + \xi_2 \sqrt{\lambda_1} + \xi_1 \sqrt{\lambda_2} + \lambda_3 \sqrt{\psi} + \sqrt{2 A_1 A_2 A_3} > 0. \tag{4.3g}$$

After enforcing the necessary condition 1, we know that $V_4 > 0$ when only the first two lines of the potential (4.1) exist; after enforcing the inequality (4.3a), we know that $V_4 > 0$ when only the third line exists. If we guarantee that the fourth line of the potential (4.1) is always positive too, then we will be sure that V_4 is always positive. We therefore have the following[8]

Sufficient condition. If, besides the two necessary conditions,

$$\xi_1 + \xi_2 > 0, \tag{4.4a}$$

$$\xi_1 \xi_2 - |\xi_3|^2 > 0, \tag{4.4b}$$

then V_4 is BFB.

Among the sets of parameters of the potential (4.1) that we have randomly generated, there were some that met both the two necessary conditions and the sufficient conditions (4.4); we have used those sets of parameters. There were many other sets that

---

[8]We thank Igor Ivanov for pointing out this sufficient condition to us.

satisfied the two necessary conditions but did not meet the sufficient conditions (4.4); for those sets, we have numerically found the absolute minimum of V_4. We have done this by using $S^2 = 1$ together with equations (3.19) and by minimizing V_4 in the domain $r^2 > 0$, $0 \le \theta \le \pi/2$, $0 \le h \le 1$, and $0 \le \alpha < 2\pi$. If the minimum of V_4 is positive, then the set of input parameters is good, else the set of input parameters is bad and one must discard it.

4.2 Unitarity conditions

There are the same five scattering channels as in the 2HDM, cf. subsection 3.1; but the channel $Q = T_3 = 0$ has an additional scattering state S^2. Additionally, there are two extra scattering channels:

- The channel $Q = 1$, $T_3 = 1/2$ with the two states aS and cS.

- The channel $Q = 0$, $T_3 = -1/2$ with the two states bS and dS.

Both these channels produce a scattering matrix

$$\mathcal{M}_4 = 2 \begin{pmatrix} \xi_1 & \xi_3 \\ \xi_3^* & \xi_2 \end{pmatrix}. \tag{4.5}$$

Channels 1 and 2 of subsection 3.1 again produce the scattering matrix (3.12). Channel 3 produces that matrix together with the additional eigenvalue I of equation (3.8). Channel 2 produces the scattering matrix (3.7a). Finally, channel 5 has the additional scattering state S^2 and therefore, instead of producing both the matrix $\mathcal{M}_1$ of equation (3.7a) and the matrix $\mathcal{M}_2$ of equation (3.7b), it produces $\mathcal{M}_1$ together with

$$\mathcal{M}_2' = \begin{pmatrix} 6\psi & \sqrt{2}\,\bar{\xi}^T \\ \sqrt{2}\,\bar{\xi} & \mathcal{M}_2 \end{pmatrix}, \quad \text{where} \quad \bar{\xi} = \begin{pmatrix} \xi_1 + \xi_2 \\ 2\,\Re\xi_3 \\ -2\,\Im\xi_3 \\ \xi_1 - \xi_2 \end{pmatrix}. \tag{4.6}$$

Thus, the unitarity conditions for the 2HDM1S are the following: both $|I|$ and the moduli of all the eigenvalues of the 2×2 matrix $\mathcal{M}_4$, of the 3×3 matrix $\mathcal{M}_3$, of the 4×4 matrix $\mathcal{M}_1$, and of the 5×5 matrix $\mathcal{M}_2'$ must be smaller than 4π.

4.3 Procedure

Just as in the previous section, we utilize the Higgs basis for the two doublets, i.e. equations (1.2) and (3.28). We also write $S = w + \sigma$, where w is the VEV of the scalar S and σ is a field. The mass terms of the scalars are

$$V = \cdots + M_C C^- C^+ + \frac{1}{2} \begin{pmatrix} H & \sigma_1 & \sigma_2 & \sigma \end{pmatrix} M \begin{pmatrix} H \\ \sigma_1 \\ \sigma_2 \\ \sigma \end{pmatrix}, \tag{4.7}$$

with

$$M = \begin{pmatrix} 2\lambda_1 v^2 & 2v^2\,\Re\lambda_6 & -2v^2\,\Im\lambda_6 & 2\sqrt{2}vw\xi_1 \\ 2v^2\,\Re\lambda_6 & M_C + (\lambda_4 + \Re\lambda_5)\,v^2 & -v^2\,\Im\lambda_5 & 2\sqrt{2}vw\,\Re\xi_3 \\ -2v^2\,\Im\lambda_6 & -v^2\,\Im\lambda_5 & M_C + (\lambda_4 - \Re\lambda_5)\,v^2 & -2\sqrt{2}vw\,\Im\xi_3 \\ 2\sqrt{2}vw\xi_1 & 2\sqrt{2}vw\,\Re\xi_3 & -2\sqrt{2}vw\,\Im\xi_3 & 4\psi w^2 \end{pmatrix}, \tag{4.8}$$

cf. equation (3.29). One diagonalizes M as

$$M = R^T \operatorname{diag}(M_1,\, M_2,\, M_3,\, M_4)\, R, \tag{4.9a}$$

$$\begin{pmatrix} H \\ \sigma_1 \\ \sigma_2 \\ \sigma \end{pmatrix} = R^T \begin{pmatrix} h_1 \\ h_2 \\ h_3 \\ h_4 \end{pmatrix}, \tag{4.9b}$$

where R is a 4×4 orthogonal matrix. The squared mass M_1 is given by equation (1.6a). Without loss of generality, $M_2 < M_3 < M_4$. Just as in the previous sections, we require

$$R_{11} \equiv c_1 > 0.9. \tag{4.10}$$

The expression for the oblique parameter T is [36]

$$T = \frac{1}{16\pi s_w^2 m_W^2} \left\{ \sum_{k=1}^{4} \left[(R_{k2})^2 + (R_{k3})^2 \right] F(M_C, M_k) \right. \tag{4.11a}$$

$$- \sum_{k=1}^{3} \sum_{k'=k+1}^{4} (R_{k2}R_{k'3} - R_{k'2}R_{k3})^2\, F(M_k, M_{k'}) \tag{4.11b}$$

$$+ 3 \sum_{k=2}^{4} (R_{k1})^2 \left[F(M_k, m_Z^2) - F(M_k, m_W^2) \right] \tag{4.11c}$$

$$\left. + 3\left(c_1^2 - 1\right) \left[F(M_1, m_Z^2) - F(M_1, m_W^2) \right] \right\}, \tag{4.11d}$$

and we demand $-0.04 < T < 0.20$.

We input random values for the 15 real parameters M_C, $\lambda_{1,2,3,4}$, $|\lambda_{5,6,7}|$, ψ, $\xi_{1,2}$, $|\xi_3|$, $\arg(\lambda_5^*\lambda_6\lambda_7)$, $\arg(\lambda_6^*\lambda_7)$, and $\arg(\lambda_6^*\xi_3)$. We moreover input M_1 and v^2 given in equations (1.6). Then,

1. We require the input parameters to satisfy the BFB conditions of subsection 4.1 — this may imply a numerical minimization of V_4 to check that $V_4 > 0$.

2. We require the input parameters to satisfy the unitarity conditions written after equation (4.6).

3. We compute the VEV w from the condition that M_1 should be an eigenvalue of the matrix M.

4. We enforce the conditions in appendix C. They guarantee that the vacuum state with $v = 174\,\text{GeV}$ and $w \neq 0$ has a lower value of the potential than all the other possible stability points of the potential.

5. We compute the full matrix M, its eigenvalues $M_{2,3,4}$, and its diagonalizing matrix R; we choose the overall sign of R such that $R_{11} \equiv c_1 > 0$.

6. We impose both the condition (4.10) and the condition that the oblique parameter T is within its experimental bounds.

7. We compute the couplings

$$g_3 = \frac{v}{\sqrt{2}} \left\{ \lambda_1 c_1^3 + (\lambda_3 + \lambda_4) c_1 \left[(R_{12})^2 + (R_{13})^2 \right] \right. \tag{4.12a}$$

$$+ c_1 \left[(R_{12})^2 - (R_{13})^2 \right] \Re\lambda_5 - 2c_1 R_{12} R_{13} \Im\lambda_5 \tag{4.12b}$$

$$+ 3c_1^2 (R_{12}\Re\lambda_6 - R_{13}\Im\lambda_6) + \left[(R_{12})^2 + (R_{13})^2 \right] (R_{12}\Re\lambda_7 - R_{13}\Im\lambda_7) \Big\} \tag{4.12c}$$

$$+ 2\psi w (R_{14})^3 + \xi_1 c_1 R_{14} \left(wc_1 + \sqrt{2}v R_{14} \right) + \xi_2 w R_{14} \left[(R_{12})^2 + (R_{13})^2 \right] \tag{4.12d}$$

$$+ \sqrt{2} R_{14} \left(v R_{14} + \sqrt{2} wc_1 \right) (R_{12}\Re\xi_3 - R_{13}\Im\xi_3), \tag{4.12e}$$

$$g_4 = \frac{\lambda_1 c_1^4}{8} + \frac{\lambda_2}{8} \left[(R_{12})^2 + (R_{13})^2 \right]^2 + \frac{\lambda_3 + \lambda_4}{4} c_1^2 \left[(R_{12})^2 + (R_{13})^2 \right] \tag{4.13a}$$

$$+ \frac{\Re\lambda_5}{4} c_1^2 \left[(R_{12})^2 - (R_{13})^2 \right] - \frac{\Im\lambda_5}{2} c_1^2 R_{12} R_{13} \tag{4.13b}$$

$$+ \frac{c_1^3}{2} (R_{12}\Re\lambda_6 - R_{13}\Im\lambda_6) + \frac{c_1 \left[(R_{12})^2 + (R_{13})^2 \right]}{2} (R_{12}\Re\lambda_7 - R_{13}\Im\lambda_7) \tag{4.13c}$$

$$+ \frac{\psi}{2} (R_{14})^4 \tag{4.13d}$$

$$+ (R_{14})^2 \left\{ \frac{\xi_1 c_1^2}{2} + \frac{\xi_2}{2} \left[(R_{12})^2 + (R_{13})^2 \right] + c_1 (R_{12}\Re\xi_3 - R_{13}\Im\xi_3) \right\}, \tag{4.13e}$$

$$g_{1CC} = \sqrt{2}v (c_1\lambda_3 + R_{12}\Re\lambda_7 - R_{13}\Im\lambda_7) + 2w\xi_2 R_{14}. \tag{4.14}$$

4.4 Results

In figure 12 we have plotted the differences among the masses of the scalars against the mass of the charged scalar. One sees that $\sqrt{M_C}$ and $\sqrt{M_3}$ cannot be more than $\sim 300\,\text{GeV}$ from each other, but $\sqrt{M_2}$ may be much smaller than both of them.

In figure 13 we present a scatter plot of the mass of the lightest non-SM neutral scalar against c_1. One sees that, contrary to what happens in the 2HDM (cf. figure 8), $\sqrt{M_2}$ may reach 1 TeV even when c_1 is as low as 0.9.

We depict in figure 14 the three- and four-Higgs couplings g_3 and g_4 in the 2HDM1S. The main difference relative to the 2HDM (cf. figure 10) is that g_4 may be much higher, just as in the SM2S. In the 2HDM1S there is no clear correlation between g_3 and g_4.
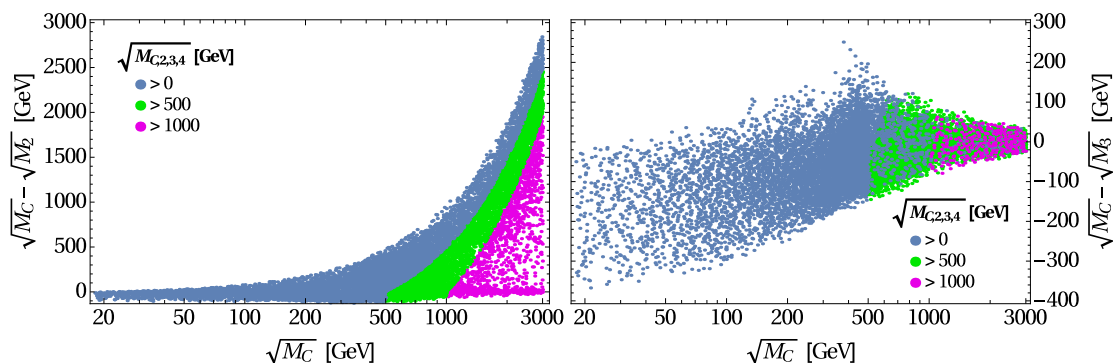
Figure 12. The differences between the masses of the two lightest non-SM neutral scalars and the mass of the charged scalar *versus* the mass of the charged scalar in the 2HDM1S. Green points have all the scalars with mass larger than $500\,\text{GeV}$; magenta points have all the scalars with mass larger than $1\,\text{TeV}$.
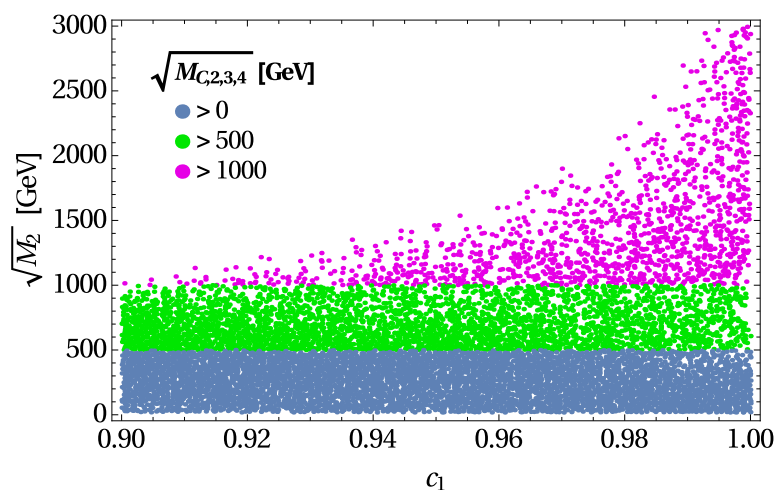

Figure 13. The mass of the lightest non-SM neutral scalar *versus* R_{11} in the 2HDM1S. Green points have all the scalars with mass larger than $500\,\text{GeV}$; magenta points have all the scalars with mass larger than $1\,\text{TeV}$.

In figure 15 we have plotted the $h_1 C^+ C^-$ coupling g_{1CC}. That coupling in the 2HDM1S may be more than two times larger than in the 2HDM; very large values of g_{1CC} occur even for c_1 very close to 1. This is because the right-hand side of equation (4.14) may be dominated by its fourth term when $w \gg v$. The first term displays the same behaviour as the corresponding term in the 2HDM, viz. it is usually positive and no larger than $1,500\,\text{GeV}$, but it is often overwhelmed by the fourth term.

5   Conclusions

In this paper we have emphasized that both the bounded-from-below (BFB) conditions and the unitarity conditions for the two-Higgs-doublet model (2HDM) are invariant under
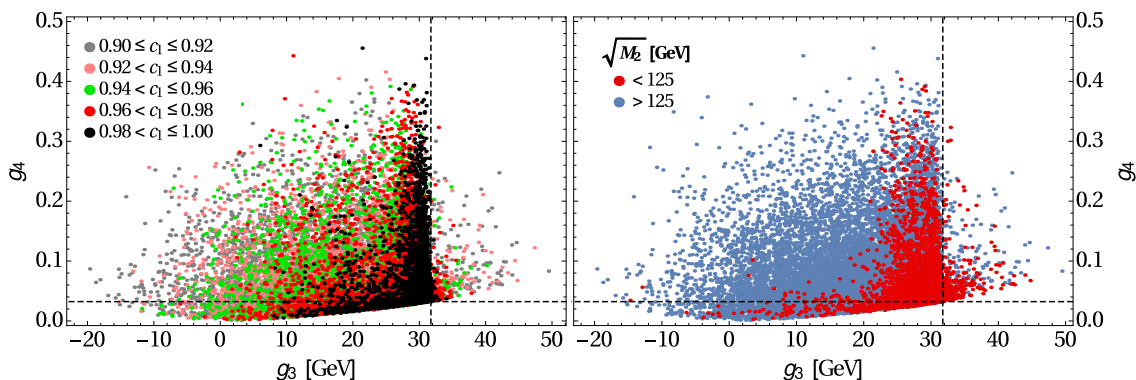
Figure 14. In the left panel, the four-Higgs coupling g_4 *versus* the three-Higgs coupling g_3 in the 2HDM1S for various values of c_1. The right panel contains the same points as the left panel but with different colours depending on whether M_2 is larger or smaller than M_1. The dashed lines mark the values of the couplings in the SM.
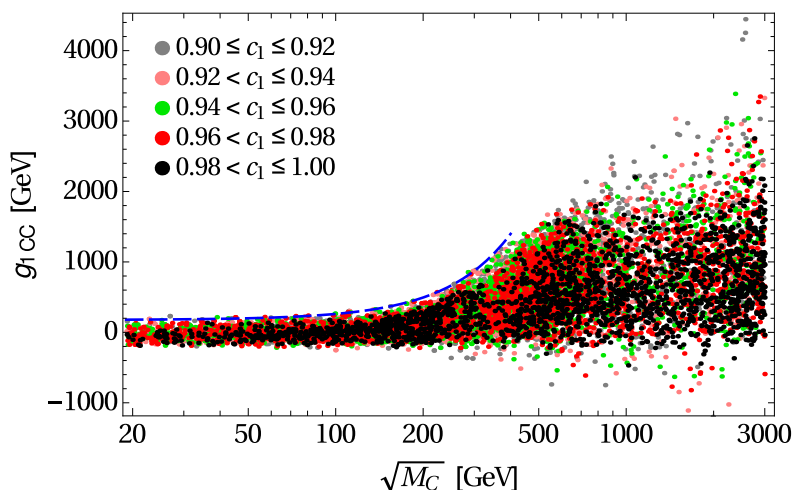

Figure 15. Scatter plot of g_{1CC} *versus* the mass of the charged scalars $C^{\pm}$ in the 2HDM1S. The blue line with equation $g_{1CC}/\text{GeV} = 174.9 + 0.138 \left(\sqrt{M_C}/\text{GeV} \right) + 0.0073 \left(M_C/\text{GeV}^2 \right)$ marks the approximate boundary of the allowed region when $\sqrt{M_C} < 400\,\text{GeV}$.

a change of the basis used for the two doublets. Therefore, one may implement those conditions directly in the Higgs basis, viz. the basis where only one doublet has vacuum expectation value. This procedure allows one to extract bounds on the masses and couplings of the scalar particles of the most general 2HDM, disregarding any symmetry that a particular 2HDM may possess. We have focussed on the three couplings $g_3 (h_1)^3$, $g_4 (h_1)^4$, and $g_{1CC} h_1 C^+ C^-$, where h_1 is the observed neutral scalar with mass $125\,\text{GeV}$ and $C^{\pm}$ are the charged scalars of the 2HDM.

We have utilized the same procedure for two other models, namely the Standard Model with the addition of two real singlets (SM2S) and the two-Higgs-doublet model with the addition of one real singlet (2HDM1S), in both cases with reflection symmetries acting on
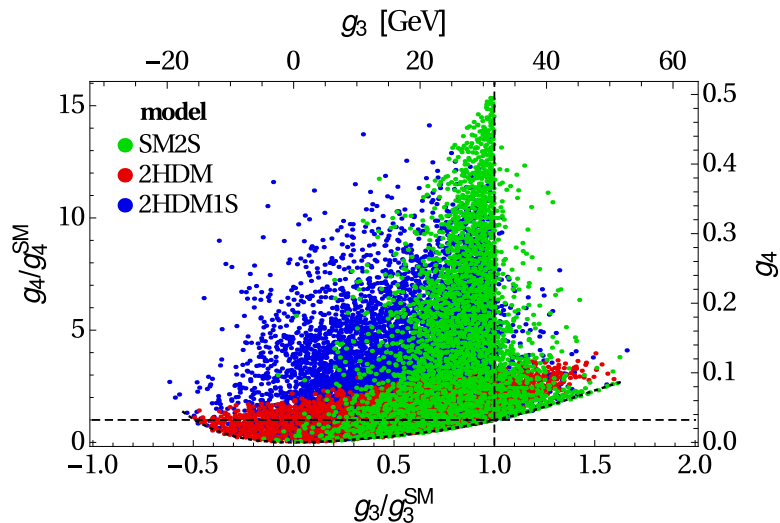
Figure 16. Scatter plot of g_4 / g_4^{SM} *versus* g_3 / g_3^{SM} in the three models that we have studied. The dashed lines mark the SM values $g_3 / g_3^{\mathrm{SM}} = g_4 / g_4^{\mathrm{SM}} = 1$. The dotted line, with equation $g_4 / g_4^{\mathrm{SM}} = 2.06 \left(g_3 / g_3^{\mathrm{SM}} \right)^2 - 2.84 \left(g_3 / g_3^{\mathrm{SM}} \right)^3 + 2.44 \left(g_3 / g_3^{\mathrm{SM}} \right)^4 - 0.67 \left(g_3 / g_3^{\mathrm{SM}} \right)^5$, marks the approximate boundary of the allowed region for $-0.6 < g_3 / g_3^{\mathrm{SM}} < 1.6$.

each of the singlets. We have found, for instance, that:

- The coupling g_3 may, in both the 2HDM and the 2HDM1S, have sign opposite to the one in the SM. On the other hand, in any of the three models that we have studied, $|g_3|$ can hardly be much larger than in the SM.

- The coupling g_4, which is always positive because of BFB, may for all practical purposes be equal to zero in all the three models. (As a matter of fact, $g_3 = g_4 = 0$ is possible in all three models.) But it may also be much larger than in the SM. A distinguished feature is that g_4 may be much larger (up to $g_4 \sim 0.5$) in the models containing singlets than in the 2HDM, wherein it can at best reach $g_4 \sim 0.13$.

- The coupling g_{1CC} may be of order TeV, but only when the mass of $C^{\pm}$ exceeds $300\,\mathrm{GeV}$; in general, a positive g_{1CC} may be larger for higher masses of $C^{\pm}$, but g_{1CC} may also be negative for any $C^{\pm}$ mass. Moreover, g_{1CC} may be more than two times larger (either positive or negative) in the 2HDM1S than in the 2HDM.

A comparison of the predictions of the three models for g_3 and g_4 is depicted in figure 16.

We emphasize that our method may be used to obtain bounds and/or correlations among other parameters and/or observables of these models. Unfortunately, it may be difficult to generalize our work to more complicated models, both because they may contain too many parameters and because it is very difficult to derive full BFB conditions for even rather simple models.

A The Higgs Singlet Model

The Higgs Singlet Model (HSM) is the Standard Model with the addition of one real scalar singlet S. We furthermore assume a symmetry $S \to -S$. The scalar potential

$$V = \mu \phi_1^\dagger \phi_1 + m^2 S^2 + \frac{\lambda}{2} \left(\phi_1^\dagger \phi_1 \right)^2 + \frac{\psi}{2} S^4 + \xi S^2 \phi_1^\dagger \phi_1 \tag{A.1}$$

has just five parameters μ, m^2, λ, ψ, and ξ. The bounded-from-below (BFB) conditions are

$$\lambda > 0, \quad \psi > 0, \quad \xi > -\sqrt{\lambda \psi}. \tag{A.2}$$

The unitarity conditions are

$$|\lambda| < 4\pi, \quad |\xi| < 2\pi, \quad \left| 3\lambda + 6\psi + \sqrt{(3\lambda - 6\psi)^2 + 16\xi^2} \right| < 8\pi. \tag{A.3}$$

We assume that ϕ_1 has VEV v and S has VEV w. We write $S = w + \sigma$ together with equation (1.2). The mass matrix for H and σ is

$$\begin{pmatrix} 2\lambda v^2 & 2\sqrt{2}\xi vw \\ 2\sqrt{2}\xi vw & 4\psi w^2 \end{pmatrix} = \begin{pmatrix} c & -s \\ s & c \end{pmatrix} \begin{pmatrix} M_1 & 0 \\ 0 & M_2 \end{pmatrix} \begin{pmatrix} c & s \\ -s & c \end{pmatrix}, \tag{A.4}$$

where $c \equiv \cos\vartheta$ and $s \equiv \sin\vartheta$. We assume $|c| > 0.9$. The oblique parameter

$$T = \frac{3s^2}{16\pi s_w^2 m_W^2} \left[F\left(M_1, m_W^2\right) - F\left(M_1, m_Z^2\right) - F\left(M_2, m_W^2\right) + F\left(M_2, m_Z^2\right) \right] \tag{A.5}$$

must satisfy $-0.04 < T < 0.20$. The three- and four-Higgs couplings are given by

$$\frac{g_3}{g_3^{\text{SM}}} = c^3 + \frac{\sqrt{2}v}{w} s^3, \tag{A.6a}$$

$$g_4 = \frac{\lambda}{8} c^4 + \frac{\psi}{2} s^4 + \frac{\xi}{2} c^2 s^2. \tag{A.6b}$$

In figure 17 we compare the predictions of the HSM and of the SM2S for g_3 and g_4. One sees that there is no substantial difference between the two models.
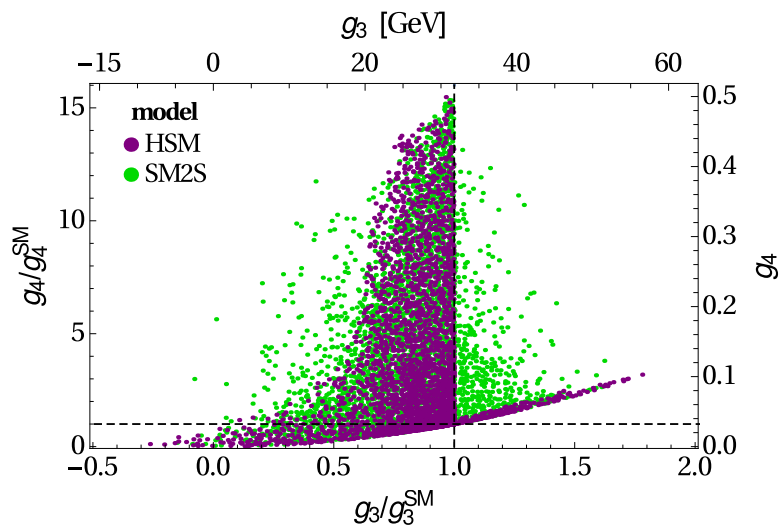
Figure 17. Scatter plot of g_4/g_4^{SM} *versus* g_3/g_3^{SM} in the HSM and in the SM2S. The dashed lines mark the Standard Model values $g_3/g_3^{\mathrm{SM}} = g_4/g_4^{\mathrm{SM}} = 1$.

B Other stability points of the SM2S potential

In this appendix we consider more carefully the various stability points of the potential of the SM2S in equation (2.1). The vacuum value of that potential is given by

$$V_0 \equiv \langle 0 \,|V|\, 0 \rangle = \mu_1 v^2 + m_1^2 w_1^2 + m_2^2 w_2^2 \tag{B.1a}$$

$$+ \frac{\lambda_1 v^4}{2} + \frac{\psi_1 w_1^4}{2} + \frac{\psi_2 w_2^4}{2} \tag{B.1b}$$

$$+ \psi_3 w_1^2 w_2^2 + \xi_1 v^2 w_1^2 + \xi_2 v^2 w_2^2. \tag{B.1c}$$

Equations (2.14) follow from the assumption that v, w_1, and w_2 are not zero. Defining

$$d \equiv \lambda_1 \psi_1 \psi_2 + 2\psi_3 \xi_1 \xi_2 - \lambda_1 \psi_3^2 - \psi_1 \xi_2^2 - \psi_2 \xi_1^2, \tag{B.2}$$

one obtains

$$V_0 = -\frac{\lambda_1 v^4}{2} - \frac{\psi_1 w_1^4}{2} - \frac{\psi_2 w_2^4}{2} - \psi_3 w_1^2 w_2^2 - \xi_1 v^2 w_1^2 - \xi_2 v^2 w_2^2 \tag{B.3a}$$

$$= \frac{1}{2d} \Big[\left(\psi_3^2 - \psi_1 \psi_2 \right) \mu_1^2 + \left(\xi_2^2 - \lambda_1 \psi_2 \right) \left(m_1^2 \right)^2 + \left(\xi_1^2 - \lambda_1 \psi_1 \right) \left(m_2^2 \right)^2 \tag{B.3b}$$

$$+ 2 \left(\xi_1 \psi_2 - \psi_3 \xi_2 \right) \mu_1 m_1^2 + 2 \left(\xi_2 \psi_1 - \psi_3 \xi_1 \right) \mu_1 m_2^2 \tag{B.3c}$$

$$+ 2 \left(\lambda_1 \psi_3 - \xi_1 \xi_2 \right) m_1^2 m_2^2 \Big]. \tag{B.3d}$$

The mass matrix M of the scalars is real and symmetric and is given in equation (2.16). We assume that M has three positive eigenvalues M_1, M_2, and M_3. It follows that all the

principal minors of M are positive.[9] (This is called 'Sylvester's criterion' [49].) Thus,

$$\lambda_1 > 0, \tag{B.4a}$$

$$\psi_1 > 0, \tag{B.4b}$$

$$\psi_2 > 0, \tag{B.4c}$$

$$\lambda_1 \psi_1 - \xi_1^2 > 0, \tag{B.4d}$$

$$\lambda_1 \psi_2 - \xi_2^2 > 0, \tag{B.4e}$$

$$\psi_1 \psi_2 - \psi_3^2 > 0, \tag{B.4f}$$

$$d > 0. \tag{B.4g}$$

These inequalities display some resemblance to the BFB conditions (2.12), (2.13).

We now consider other stability points of the potential where either v or w_1 or w_2 vanish.

1. There is a stability point where $w_1 = w_2 = 0$. At that point the potential has the value

$$V^{(1)} \equiv -\frac{\mu_1^2}{2\lambda_1}. \tag{B.5}$$

2. Similarly, there are stability points where either $v = w_1 = 0$ or $v = w_2 = 0$. At those two points the values of the potential are, respectively,

$$V^{(2)} \equiv -\frac{\left(m_2^2\right)^2}{2\psi_2}, \tag{B.6a}$$

$$V^{(3)} \equiv -\frac{\left(m_1^2\right)^2}{2\psi_1}. \tag{B.6b}$$

3. There is a stability point of the potential where $v = 0$ but w_1 and w_2 are nonzero. At that point the potential takes the value

$$V^{(4)} \equiv \frac{-\psi_2 \left(m_1^2\right)^2 - \psi_1 \left(m_2^2\right)^2 + 2\psi_3 m_1^2 m_2^2}{2 \left(\psi_1 \psi_2 - \psi_3^2\right)}. \tag{B.7}$$

4. Similarly, there is a stability point where $w_1 = 0$ but $v \neq 0$ and $w_2 \neq 0$. At that point the value of the potential is

$$V^{(5)} \equiv \frac{-\psi_2 \mu_1^2 - \lambda_1 \left(m_2^2\right)^2 + 2\xi_2 \mu_1 m_2^2}{2 \left(\lambda_1 \psi_2 - \xi_2^2\right)}. \tag{B.8}$$

5. Finally, there is another stability point with value

$$V^{(6)} \equiv \frac{-\psi_1 \mu_1^2 - \lambda_1 \left(m_1^2\right)^2 + 2\xi_1 \mu_1 m_1^2}{2 \left(\lambda_1 \psi_1 - \xi_1^2\right)} \tag{B.9}$$

of the potential.

---

[9]The principal minors of a square matrix are the determinants of its principal submatrices.

From inequalities (B.4c) and (B.4f) it follows that $V^{(4)} \leq V^{(2)}$ is equivalent to

$$\psi_2 \left[-\psi_2 \left(m_1^2\right)^2 - \psi_1 \left(m_2^2\right)^2 + 2\psi_3 m_1^2 m_2^2 \right] \leq \left(\psi_3^2 - \psi_1\psi_2\right)\left(m_2^2\right)^2, \qquad \text{(B.10)}$$

which in turn is equivalent to

$$- \left(\psi_2 m_1^2 - \psi_3 m_2^2\right)^2 \leq 0, \qquad \text{(B.11)}$$

and this is obvioulsy true. One thus concludes that $V^{(4)}$ can never be larger than $V^{(2)}$. In similar fashion one finds that

$$V^{(4)} \leq V^{(2)}, \qquad \text{(B.12a)}$$

$$V^{(4)} \leq V^{(3)}, \qquad \text{(B.12b)}$$

$$V^{(5)} \leq V^{(1)}, \qquad \text{(B.12c)}$$

$$V^{(5)} \leq V^{(2)}, \qquad \text{(B.12d)}$$

$$V^{(6)} \leq V^{(1)}, \qquad \text{(B.12e)}$$

$$V^{(6)} \leq V^{(3)}. \qquad \text{(B.12f)}$$

Next consider the inequality $V_0 \leq V^{(4)}$. Because of (B.4f) and (B.4g), it is equivalent to

$$\left(\psi_1\psi_2 - \psi_3^2\right) \left[\left(\psi_3^2 - \psi_1\psi_2\right)\mu_1^2 + \left(\xi_2^2 - \lambda_1\psi_2\right)\left(m_1^2\right)^2 \right. \qquad \text{(B.13a)}$$

$$+ \left(\xi_1^2 - \lambda_1\psi_1\right)\left(m_2^2\right)^2 + 2\left(\xi_1\psi_2 - \psi_3\xi_2\right)\mu_1 m_1^2 \qquad \text{(B.13b)}$$

$$+2\left(\xi_2\psi_1 - \psi_3\xi_1\right)\mu_1 m_2^2 + 2\left(\lambda_1\psi_3 - \xi_1\xi_2\right)m_1^2 m_2^2 \right] \leq d\left[-\psi_2\left(m_1^2\right)^2 \right. \qquad \text{(B.13c)}$$

$$- \psi_1\left(m_2^2\right)^2 \qquad \text{(B.13d)}$$

$$\left. +2\psi_3 m_1^2 m_2^2 \right]. \qquad \text{(B.13e)}$$

Introducing the expression for d in equation (B.2), one finds that the inequality (B.13) is equivalent to

$$\left(\psi_1\psi_1 - \psi_3^2\right) \left[\left(\psi_3^2 - \psi_1\psi_2\right)\mu_1^2 + 2\left(\xi_1\psi_2 - \psi_3\xi_2\right)\mu_1 m_1^2 \right. \qquad \text{(B.14a)}$$

$$+2\left(\xi_2\psi_1 - \psi_3\xi_1\right)\mu_1 m_2^2 \right] - \left(m_1^2\right)^2\left(\psi_2\xi_1 - \psi_3\xi_2\right)^2 \qquad \text{(B.14b)}$$

$$- \left(m_2^2\right)^2\left(\psi_1\xi_2 - \psi_3\xi_1\right)^2 - 2m_1^2 m_2^2\left(\psi_2\xi_1 - \psi_3\xi_2\right)\left(\psi_1\xi_2 - \psi_3\xi_1\right) \leq 0. \qquad \text{(B.14c)}$$

This may be written as

$$\left[\left(\psi_3^2 - \psi_1\psi_2\right)\mu_1 + \left(\psi_2\xi_1 - \psi_3\xi_2\right)m_1^2 + \left(\psi_1\xi_2 - \psi_3\xi_1\right)m_2^2 \right]^2 \geq 0, \qquad \text{(B.15)}$$

which is of course true. In similar fashion one obtains that

$$V_0 \leq V^{(4)}, \qquad \text{(B.16a)}$$

$$V_0 \leq V^{(5)}, \qquad \text{(B.16b)}$$

$$V_0 \leq V^{(6)}. \qquad \text{(B.16c)}$$

We have thus demonstrated that, because of our assumption that all three eigenvalues of the matrix M are positive, V_0 is smaller than $V^{1,2,3,4,5,6}$, viz. the stability point of V with nonzero v, w_1, and w_2 is the vacuum.

This result may be easily understood in the following way. The potential (2.1) of the SM2S may be rewritten

$$V = \frac{1}{2} X^T \Lambda X + V_0, \tag{B.17}$$

where V_0 is the vacuum expectation value of the potential given in equation (B.3a) and

$$X = \begin{pmatrix} \phi_1^\dagger \phi_1 - v^2 \\ S_1^2 - w_1^2 \\ S_2^2 - w_2^2 \end{pmatrix}, \quad \Lambda = \begin{pmatrix} \lambda_1 & \xi_1 & \xi_2 \\ \xi_1 & \psi_1 & \psi_3 \\ \xi_2 & \psi_3 & \psi_2 \end{pmatrix}. \tag{B.18}$$

We assume that the point $X = \begin{pmatrix} 0, & 0, & 0 \end{pmatrix}^T$ is a local minimum of the potential V. Then, since the potential in equation (B.17) is a quadratic form is X, the point $X = \begin{pmatrix} 0, & 0, & 0 \end{pmatrix}^T$ must also be the *global* minimum of V.[10]

C Global minimum conditions for the 2HDM1S

In the 2HDM1S, we define $q_1 \equiv \phi_1^\dagger \phi_1$, $q_2 \equiv \phi_2^\dagger \phi_2$, $z \equiv \phi_1^\dagger \phi_2$, $z^* \equiv \phi_2^\dagger \phi_1$,[11] and $q_3 \equiv S^2$. Note that

$$q_1 \geq 0, \quad q_2 \geq 0, \quad |z|^2 \leq q_1 q_2, \quad q_3 \geq 0. \tag{C.1}$$

We define the column vector $X = \begin{pmatrix} q_1, & q_2, & z, & z^*, & q_3 \end{pmatrix}^T$. The scalar potential of the 2HDM1S may then be written as

$$V = Y^T X + \frac{1}{2} X^T \Lambda X, \tag{C.2}$$

where

$$Y = \begin{pmatrix} \mu_1 \\ \mu_2 \\ \mu_3 \\ \mu_3^* \\ \mu_4 \end{pmatrix}, \quad \Lambda = \begin{pmatrix} \lambda_1 & \lambda_3 & \lambda_6 & \lambda_6^* & \xi_1 \\ \lambda_3 & \lambda_2 & \lambda_7 & \lambda_7^* & \xi_2 \\ \lambda_6 & \lambda_7 & \lambda_5 & \lambda_4 & \xi_3 \\ \lambda_6^* & \lambda_7^* & \lambda_4 & \lambda_5^* & \xi_3^* \\ \xi_1 & \xi_2 & \xi_3 & \xi_3^* & \psi \end{pmatrix}. \tag{C.3}$$

The coefficients μ_1, μ_2, μ_3, and μ_4 contained in the column vector Y have squared-mass dimension; μ_3 is in general complex while μ_1, μ_2, and μ_4 are real. The coefficients contained in the symmetric matrix Λ are treated by us as an input, cf. section 4.3. Since we study the 2HDM1S in the Higgs basis, where ϕ_2 has zero VEV, in the vacuum one has $q_2 = z = z^* = 0$, $q_1 = v^2$, and $q_3 = w^2$; the vacuum expectation value of the potential is

$$V_0 \equiv \langle 0 | V | 0 \rangle = \mu_1 v^2 + \mu_4 w^2 + \frac{\lambda_1 v^4}{2} + \frac{\psi w^4}{2} + \xi_1 v^2 w^2. \tag{C.4}$$

---

[10]We thank Igor Ivanov for presenting this argument to us.

[11]Since we only analyze the potential at the classical level, we simplify the notation by treating the fields as c-numbers instead of q-numbers.

It follows that

$$\mu_1 = -\lambda_1 v^2 - \xi_1 w^2, \tag{C.5a}$$

$$\mu_4 = -\xi_1 v^2 - \psi w^2. \tag{C.5b}$$

Solving for v^2 and w^2 the system (C.5) and plugging the solution into equation (C.4), one obtains

$$V_0 = \frac{-\psi \left(\mu_1\right)^2 - \lambda_1 \left(\mu_4\right)^2 + 2\xi_1 \mu_1 \mu_4}{2 \left[\psi \lambda_1 - \left(\xi_1\right)^2\right]}. \tag{C.6}$$

Moreover, in the Higgs basis

$$\mu_2 = M_C - \lambda_3 v^2 - \xi_2 w^2, \tag{C.7a}$$

$$\mu_3 = -\lambda_6 v^2 - \xi_3 w^2. \tag{C.7b}$$

In equation (C.7a), M_C is the mass of the charged scalar; we treat it as an input, just as v and w.[12] By using equations (C.5) and (C.7) we find the values of μ_1, μ_2, μ_3, and μ_4 from the input.

We want to check that, for each set of input parameters (i.e. $\lambda_{1,...,7}$, $\xi_{1,2,3}$, ψ, v, w, and M_C) in our data set, the state that we *assume* to be the vacuum, characterized by $q_2 = z = z^* = 0$, is *indeed* the *global* minimum of the potential. In order to do this we must consider all the other possible stability points of the potential and check that the value of the potential at each of those points is larger than V_0 in equation (C.6). The stability points may either be inside the domain defined by equations (C.1) or they may lie on a boundary of that domain. There is only one possible stability point inside the domain; deriving equation (C.2) relative to X, we find that it is given by

$$X \equiv X^{(1)} = -\Lambda^{-1} Y, \tag{C.8a}$$

$$V \equiv V^{(1)} = -\frac{1}{2} Y^T \Lambda^{-1} Y. \tag{C.8b}$$

For each set of input parameters, we have computed the column vector $X^{(1)}$ by using equation (C.8a). If that vector happened to be inside the domain, viz. if $X_1^{(1)} > 0$, $X_2^{(1)} > 0$, $\left|X_3^{(1)}\right|^2 < X_1^{(1)} X_2^{(1)}$, and $X_4^{(1)} > 0$, then we computed $V^{(1)}$ by using equation (C.8b). We checked whether $V^{(1)} > V_0$; if the latter condition did *not* hold, then we discarded that set of input parameters.

Next we have considered the various possible stability points on boundaries of the domain. Firstly there is the boundary with $q_3 = 0$ but $q_1 > 0$, $q_2 > 0$, and $|z|^2 < q_1 q_2$. In that case one has

$$V = \bar{Y}^T \bar{X} + \frac{1}{2} \bar{X}^T \bar{\Lambda} \bar{X}, \tag{C.9}$$

---

[12]More exactly, we input $v = 174 \, \text{GeV}$ and the squared mass $M_1 = (125 \, \text{GeV})^2$ of one of the scalars, and we derive the value of w therefrom.

where

$$\bar{X} = \begin{pmatrix} q_1 \\ q_2 \\ z \\ z^* \end{pmatrix}, \quad \bar{Y} = \begin{pmatrix} \mu_1 \\ \mu_2 \\ \mu_3 \\ \mu_3^* \end{pmatrix}, \quad \bar{\Lambda} = \begin{pmatrix} \lambda_1 & \lambda_3 & \lambda_6 & \lambda_6^* \\ \lambda_3 & \lambda_2 & \lambda_7 & \lambda_7^* \\ \lambda_6 & \lambda_7 & \lambda_5 & \lambda_4 \\ \lambda_6^* & \lambda_7^* & \lambda_4 & \lambda_5^* \end{pmatrix}. \tag{C.10}$$

There is one possible stability point with

$$\bar{X} \equiv \bar{X}^{(2)} = -\bar{\Lambda}^{-1}\bar{Y}, \tag{C.11a}$$

$$V \equiv V^{(2)} = -\frac{1}{2}\bar{Y}^T\bar{\Lambda}^{-1}\bar{Y}. \tag{C.11b}$$

For each set of input parameters, we have computed the column vector $\bar{X}^{(2)}$ by using equation (C.11a). Whenever that vector happened to fulfil $\bar{X}_1^{(2)} > 0$, $\bar{X}_2^{(2)} > 0$, and $\left|\bar{X}_3^{(2)}\right|^2 < \bar{X}_1^{(2)}\bar{X}_2^{(2)}$, we computed $V^{(2)}$ by using equation (C.11b). We checked whether $V^{(2)} > V_0$; if that condition did not hold, then we discarded the set of input parameters.

Secondly we have checked a possible stability point with null q_1 (and z) instead of null q_2 (and z). In analogy with equations (C.5) and (C.6), in that case one has

$$q_2 = \frac{-\psi\mu_2 + \xi_2\mu_4}{\psi\lambda_2 - (\xi_2)^2}, \tag{C.12a}$$

$$q_3 = \frac{\xi_2\mu_2 - \lambda_2\mu_4}{\psi\lambda_2 - (\xi_2)^2}, \tag{C.12b}$$

$$V \equiv V^{(3)} = \frac{-\psi(\mu_2)^2 - \lambda_2(\mu_4)^2 + 2\xi_2\mu_2\mu_4}{2\left[\psi\lambda_2 - (\xi_2)^2\right]}. \tag{C.12c}$$

For each set of parameters, we have computed q_2 and q_3 through equations (C.12a) and (C.12b), respectively. Whenever q_2 and q_3 were both positive, we have computed $V^{(3)}$ through equation (C.12c); if $V^{(3)} < V_0$, then we discarded the set of parameters.

Thirdly, we have considered the following possible stability points on boundaries of the domain:

1. The point $q_1 = q_2 = z = q_3 = 0$ has $V = 0$, Therefore, when $V_0 > 0$ we have discarded the set of parameters.

2. When $q_1 = q_2 = z = 0$ but $q_3 \neq 0$, there is a stability point featuring

$$q_3 = -\frac{\mu_4}{\psi}, \tag{C.13a}$$

$$V \equiv V^{(4)} = -\frac{(\mu_4)^2}{2\psi}. \tag{C.13b}$$

Whenever q_3 in equation (C.13a) happened to be positive and simultaneously $V^{(4)}$ in equation (C.13b) was smaller then V_0, we have discarded the set of parameters.

3. When $q_1 = q_3 = z = 0$ but $q_2 \neq 0$, there is a stability point featuring

$$q_2 = -\frac{\mu_2}{\lambda_2}, \tag{C.14a}$$

$$V \equiv V^{(5)} = -\frac{(\mu_2)^2}{2\lambda_2}. \tag{C.14b}$$

Whenever q_2 in equation (C.14a) happened to be positive and simultaneously $V^{(5)}$ in equation (C.14b) was smaller then V_0, we have discarded the set of parameters.

4. When $q_2 = q_3 = z = 0$ but $q_1 \neq 0$, there is a stability point featuring

$$q_1 = -\frac{\mu_1}{\lambda_1}, \tag{C.15a}$$

$$V \equiv V^{(6)} = -\frac{(\mu_1)^2}{2\lambda_1}. \tag{C.15b}$$

Whenever q_1 in equation (C.15a) happened to be positive and simultaneously $V^{(6)}$ in equation (C.15b) was smaller then V_0, we have discarded the set of parameters.

All the above tests are easily applied. The awkward tests involve the boundaries where $|z|^2 = q_1 q_2$. In that case one writes $z = e^{i\theta}\sqrt{q_1 q_2}$ to obtain

$$V \equiv \hat{V}_0 = \mu_1 q_1 + \mu_2 q_2 + 2\,\Re\left(\mu_3 e^{i\theta}\right)\sqrt{q_1 q_2} + \mu_4 q_3 \tag{C.16a}$$

$$+ \frac{\lambda_1}{2}(q_1)^2 + \frac{\lambda_2}{2}(q_2)^2 + \frac{\psi}{2}(q_3)^2 + \left[\lambda_3 + \lambda_4 + \Re\left(\lambda_5 e^{2i\theta}\right)\right]q_1 q_2 \tag{C.16b}$$

$$+ 2\,\Re\left(\lambda_6 e^{i\theta}\right)q_1\sqrt{q_1 q_2} + 2\,\Re\left(\lambda_7 e^{i\theta}\right)q_2\sqrt{q_1 q_2} \tag{C.16c}$$

$$+ \xi_1 q_1 q_3 + \xi_2 q_2 q_3 + 2\,\Re\left(\xi_3 e^{i\theta}\right)q_3\sqrt{q_1 q_2}. \tag{C.16d}$$

Deriving $\hat{V}_0$ in equation (C.16) relative to q_1, q_2, q_3, and θ one obtains the stability equations

$$0 = \mu_1 + \Re\left(\mu_3 e^{i\theta}\right)\sqrt{\frac{q_2}{q_1}} + \lambda_1 q_1 + \left[\lambda_3 + \lambda_4 + \Re\left(\lambda_5 e^{2i\theta}\right)\right]q_2 \tag{C.17a}$$

$$+ 3\,\Re\left(\lambda_6 e^{i\theta}\right)\sqrt{q_1 q_2} + \Re\left(\lambda_7 e^{i\theta}\right)q_2\sqrt{\frac{q_2}{q_1}} \tag{C.17b}$$

$$+ \xi_1 q_3 + \Re\left(\xi_3 e^{i\theta}\right)q_3\sqrt{\frac{q_2}{q_1}}, \tag{C.17c}$$

$$0 = \mu_2 + \Re\left(\mu_3 e^{i\theta}\right)\sqrt{\frac{q_1}{q_2}} + \lambda_2 q_2 + \left[\lambda_3 + \lambda_4 + \Re\left(\lambda_5 e^{2i\theta}\right)\right]q_1 \tag{C.17d}$$

$$+ \Re\left(\lambda_6 e^{i\theta}\right)q_1\sqrt{\frac{q_1}{q_2}} + 3\,\Re\left(\lambda_7 e^{i\theta}\right)\sqrt{q_1 q_2} \tag{C.17e}$$

$$+ \xi_2 q_3 + \Re\left(\xi_3 e^{i\theta}\right)q_3\sqrt{\frac{q_1}{q_2}}, \tag{C.17f}$$

$$0 = \mu_4 + \psi q_3 + \xi_1 q_1 + \xi_2 q_2 + 2\,\Re\left(\xi_3 e^{i\theta}\right)\sqrt{q_1 q_2}, \tag{C.17g}$$

$$0 = \Im\left(\mu_3 e^{i\theta}\right) + \Im\left(\lambda_5 e^{2i\theta}\right)\sqrt{q_1 q_2} \tag{C.17h}$$

$$+ \Im\left(\lambda_6 e^{i\theta}\right)q_1 + \Im\left(\lambda_7 e^{i\theta}\right)q_2 + \Im\left(\xi_3 e^{i\theta}\right)q_3. \tag{C.17i}$$

For each set of parameters of the potential, we have searched for solutions, i.e. for $q_1 > 0$, $q_2 > 0$, $q_3 > 0$, and a phase θ satisfying the system (C.17) of four equations. (This proved to be a highly nontrivial task.) Whenever we found a solution, we computed $\hat{V}_0$ through equation (C.16) and checked whether $\hat{V}_0 < V_0$; when that happened for at least one solution of (C.17), we have discarded the corresponding set of parameters.

One must also consider the domain border $|z|^2 = q_1 q_2$ and $q_3 = 0$. In that case one must solve the simpler system of equations

$$0 = \mu_1 + \Re\left(\mu_3 e^{i\theta}\right)\sqrt{\frac{q_2}{q_1}} + \lambda_1 q_1 + \left[\lambda_3 + \lambda_4 + \Re\left(\lambda_5 e^{2i\theta}\right)\right] q_2 \tag{C.18a}$$

$$+ 3\,\Re\left(\lambda_6 e^{i\theta}\right)\sqrt{q_1 q_2} + \Re\left(\lambda_7 e^{i\theta}\right) q_2 \sqrt{\frac{q_2}{q_1}}, \tag{C.18b}$$

$$0 = \mu_2 + \Re\left(\mu_3 e^{i\theta}\right)\sqrt{\frac{q_1}{q_2}} + \lambda_2 q_2 + \left[\lambda_3 + \lambda_4 + \Re\left(\lambda_5 e^{2i\theta}\right)\right] q_1 \tag{C.18c}$$

$$+ \Re\left(\lambda_6 e^{i\theta}\right) q_1 \sqrt{\frac{q_1}{q_2}} + 3\,\Re\left(\lambda_7 e^{i\theta}\right)\sqrt{q_1 q_2}, \tag{C.18d}$$

$$0 = \Im\left(\mu_3 e^{i\theta}\right) + \Im\left(\lambda_5 e^{2i\theta}\right)\sqrt{q_1 q_2} + \Im\left(\lambda_6 e^{i\theta}\right) q_1 + \Im\left(\lambda_7 e^{i\theta}\right) q_2. \tag{C.18e}$$

For each set of parameters, whenever we found a solution $q_1 > 0$, $q_2 > 0$, and θ of equations (C.18) we computed

$$\tilde{V}_0 = \mu_1 q_1 + \mu_2 q_2 + 2\,\Re\left(\mu_3 e^{i\theta}\right)\sqrt{q_1 q_2} \tag{C.19a}$$

$$+ \frac{\lambda_1}{2}\left(q_1\right)^2 + \frac{\lambda_2}{2}\left(q_2\right)^2 + \left[\lambda_3 + \lambda_4 + \Re\left(\lambda_5 e^{2i\theta}\right)\right] q_1 q_2 \tag{C.19b}$$

$$+ 2\,\Re\left(\lambda_6 e^{i\theta}\right) q_1 \sqrt{q_1 q_2} + 2\,\Re\left(\lambda_7 e^{i\theta}\right) q_2 \sqrt{q_1 q_2}. \tag{C.19c}$$

If $\tilde{V}_0 < V_0$ for any solution of equations (C.18), then we discarded the set of input parameters.

By applying all the tests in this appendix, we have eliminated about half of our initial set of sets of input parameters. Thus, the tests in this appendix prove crucial in the correct analysis of the 2HDM1S.

We have also applied the tests in this appendix, with the necessary simplifications, to the case of the 2HDM [50]. In particular, in that case we do not have to solve the very complicated system of four equations (C.17), we only have to solve the much easier system of three equations (C.18). We have checked that the tests in this appendix yield, for the 2HDM, exactly the same result as the much simpler method described in the paragraph between equations (3.32) and (3.33).

References

[1] ATLAS collaboration, *Observation of a new particle in the search for the Standard Model Higgs boson with the ATLAS detector at the LHC*, [*Phys. Lett.* **B 716** (2012) 1](https://doi.org/10.1016/j.physletb.2012.08.020) [[arXiv:1207.7214](https://arxiv.org/abs/1207.7214)] [[INSPIRE](https://inspirehep.net/search?p=arXiv:1207.7214)].

[2] CMS collaboration, *Observation of a new boson at a mass of 125 GeV with the CMS experiment at the LHC*, [*Phys. Lett.* **B 716** (2012) 30](https://doi.org/10.1016/j.physletb.2012.08.021) [[arXiv:1207.7235](https://arxiv.org/abs/1207.7235)] [[INSPIRE](https://inspirehep.net/search?p=arXiv:1207.7235)].

[3] I.P. Ivanov, *Building and testing models with extended Higgs sectors*, [*Prog. Part. Nucl. Phys.* **95** (2017) 160](https://doi.org/10.1016/j.ppnp.2017.03.001) [[arXiv:1702.03776](https://arxiv.org/abs/1702.03776)] [[INSPIRE](https://inspirehep.net/search?p=arXiv:1702.03776)].

[4] PARTICLE DATA GROUP collaboration, C. Patrignani et al., *Review of Particle Physics*, [*Chin. Phys.* **C 40** (2016) 100001](https://doi.org/10.1088/1674-1137/40/10/100001) [[INSPIRE](https://inspirehep.net/search?p=Chin.Phys.,C40,100001)].

[5] J. Baglio, O. Eberhardt, U. Nierste and M. Wiebusch, *Benchmarks for Higgs Pair Production and Heavy Higgs boson Searches in the Two-Higgs-Doublet Model of Type II*, [*Phys. Rev.* **D 90** (2014) 015008](https://doi.org/10.1103/PhysRevD.90.015008) [[arXiv:1403.1264](https://arxiv.org/abs/1403.1264)] [[INSPIRE](https://inspirehep.net/search?p=arXiv:1403.1264)].

[6] L. Wu, J.M. Yang, C.-P. Yuan and M. Zhang, *Higgs self-coupling in the MSSM and NMSSM after the LHC Run 1*, [*Phys. Lett.* **B 747** (2015) 378](https://doi.org/10.1016/j.physletb.2015.06.020) [[arXiv:1504.06932](https://arxiv.org/abs/1504.06932)] [[INSPIRE](https://inspirehep.net/search?p=arXiv:1504.06932)].

[7] L. Bian and N. Chen, *Higgs pair productions in the CP-violating two-Higgs-doublet model*, [*JHEP* **09** (2016) 069](https://doi.org/10.1007/JHEP09(2016)069) [[arXiv:1607.02703](https://arxiv.org/abs/1607.02703)] [[INSPIRE](https://inspirehep.net/search?p=arXiv:1607.02703)].

[8] N. Chakrabarty and B. Mukhopadhyaya, *High-scale validity of a two Higgs doublet scenario: predicting collider signals*, [*Phys. Rev.* **D 96** (2017) 035028](https://doi.org/10.1103/PhysRevD.96.035028) [[arXiv:1702.08268](https://arxiv.org/abs/1702.08268)] [[INSPIRE](https://inspirehep.net/search?p=arXiv:1702.08268)].

[9] N.F. Bell, G. Busoni and I.W. Sanderson, *Self-consistent Dark Matter Simplified Models with an s-channel scalar mediator*, [*JCAP* **03** (2017) 015](https://doi.org/10.1088/1475-7516/2017/03/015) [[arXiv:1612.03475](https://arxiv.org/abs/1612.03475)] [[INSPIRE](https://inspirehep.net/search?p=arXiv:1612.03475)].

[10] N.F. Bell, G. Busoni and I.W. Sanderson, *Two Higgs Doublet Dark Matter Portal*, [*JCAP* **01** (2018) 015](https://doi.org/10.1088/1475-7516/2018/01/015) [[arXiv:1710.10764](https://arxiv.org/abs/1710.10764)] [[INSPIRE](https://inspirehep.net/search?p=arXiv:1710.10764)].

[11] M. Bauer, U. Haisch and F. Kahlhoefer, *Simplified dark matter models with two Higgs doublets: I. Pseudoscalar mediators*, [*JHEP* **05** (2017) 138](https://doi.org/10.1007/JHEP05(2017)138) [[arXiv:1701.07427](https://arxiv.org/abs/1701.07427)] [[INSPIRE](https://inspirehep.net/search?p=arXiv:1701.07427)].

[12] C.-F. Chang, X.-G. He and J. Tandean, *Two-Higgs-Doublet-Portal Dark-Matter Models in Light of Direct Search and LHC Data*, [*JHEP* **04** (2017) 107](https://doi.org/10.1007/JHEP04(2017)107) [[arXiv:1702.02924](https://arxiv.org/abs/1702.02924)] [[INSPIRE](https://inspirehep.net/search?p=arXiv:1702.02924)].

[13] M. Gorbahn and U. Haisch, *Indirect probes of the trilinear Higgs coupling: $gg \to h$ and $h \to \gamma\gamma$*, [*JHEP* **10** (2016) 094](https://doi.org/10.1007/JHEP10(2016)094) [[arXiv:1607.03773](https://arxiv.org/abs/1607.03773)] [[INSPIRE](https://inspirehep.net/search?p=arXiv:1607.03773)].

[14] W. Bizoń, M. Gorbahn, U. Haisch and G. Zanderighi, *Constraints on the trilinear Higgs coupling from vector boson fusion and associated Higgs production at the LHC*, [*JHEP* **07** (2017) 083](https://doi.org/10.1007/JHEP07(2017)083) [[arXiv:1610.05771](https://arxiv.org/abs/1610.05771)] [[INSPIRE](https://inspirehep.net/search?p=arXiv:1610.05771)].

[15] ATLAS collaboration, *Search for pair production of Higgs bosons in the $b\bar{b}b\bar{b}$ final state using proton−proton collisions at $\sqrt{s} = 13$ TeV with the ATLAS detector*, [ATLAS-CONF-2016-049](https://cds.cern.ch/record/2206131).

[16] S.D. Rindani and B. Singh, *Indirect measurement of triple-Higgs coupling at an electron-positron collider with polarized beams*, [arXiv:1805.03417](https://arxiv.org/abs/1805.03417) [[INSPIRE](https://inspirehep.net/search?p=arXiv:1805.03417)].

[17] G.D. Kribs, A. Maier, H. Rzehak, M. Spannowsky and P. Waite, *Electroweak oblique parameters as a probe of the trilinear Higgs boson self-interaction*, *Phys. Rev.* **D 95** (2017) 093004 [arXiv:1702.07678] [INSPIRE].

[18] G. Degrassi, P.P. Giardino, F. Maltoni and D. Pagani, *Probing the Higgs self coupling via single Higgs production at the LHC*, *JHEP* **12** (2016) 080 [arXiv:1607.04251] [INSPIRE].

[19] G. Degrassi, M. Fedele and P.P. Giardino, *Constraints on the trilinear Higgs self coupling from precision observables*, *JHEP* **04** (2017) 155 [arXiv:1702.01737] [INSPIRE].

[20] L. Di Luzio, R. Gröber and M. Spannowsky, *Maxi-sizing the trilinear Higgs self-coupling: how large could it be?*, *Eur. Phys. J.* **C 77** (2017) 788 [arXiv:1704.02311] [INSPIRE].

[21] D. Jurčiukonis and L. Lavoura, *Lepton mixing and the charged-lepton mass ratios*, *JHEP* **03** (2018) 152 [arXiv:1712.04292] [INSPIRE].

[22] R. Gonçalo, *Latest Higgs results from ATLAS*, talk at *The Workshop on Multi-Higgs Models*, Lisbon, Portugal, 4–7 September 2018 [http://cftp.ist.utl.pt].

[23] P. Silva, *Latest from CMS on the exploration of the Higgs sector*, talk at *The Workshop on Multi-Higgs Models*, Lisbon, Portugal, 4–7 September 2018 [http://cftp.ist.utl.pt].

[24] S. Di Vita et al., *A global view on the Higgs self-coupling at lepton colliders*, *JHEP* **02** (2018) 178 [arXiv:1711.03978] [INSPIRE].

[25] T. Plehn and M. Rauch, *The quartic Higgs coupling at hadron colliders*, *Phys. Rev.* **D 72** (2005) 053008 [hep-ph/0507321] [INSPIRE].

[26] T. Liu, K.-F. Lyu, J. Ren and H.X. Zhu, *Probing the quartic Higgs boson self-interaction*, *Phys. Rev.* **D 98** (2018) 093004 [arXiv:1803.04359] [INSPIRE].

[27] A. Abada, D. Ghaffor and S. Nasri, *A Two-Singlet Model for Light Cold Dark Matter*, *Phys. Rev.* **D 83** (2011) 095021 [arXiv:1101.0365] [INSPIRE].

[28] A. Ahriche, A. Arhrib and S. Nasri, *Higgs Phenomenology in the Two-Singlet Model*, *JHEP* **02** (2014) 042 [arXiv:1309.5615] [INSPIRE].

[29] B. Grzadkowski and D. Huang, *Spontaneous CP-Violating Electroweak Baryogenesis and Dark Matter from a Complex Singlet Scalar*, *JHEP* **08** (2018) 135 [arXiv:1807.06987] [INSPIRE].

[30] A. Arhrib and M. Maniatis, *The two-real-singlet Dark Matter model*, arXiv:1807.03554 [INSPIRE].

[31] M.D. Goodsell and F. Staub, *Unitarity constraints on general scalar couplings with SARAH*, *Eur. Phys. J.* **C 78** (2018) 649 [arXiv:1805.07306] [INSPIRE].

[32] M.D. Goodsell and F. Staub, *Improved unitarity constraints in Two-Higgs-Doublet-Models*, arXiv:1805.07310 [INSPIRE].

[33] M.P. Bento, H.E. Haber, J.C. Romão and J.P. Silva, *Multi-Higgs doublet models: physical parametrization, sum rules and unitarity bounds*, *JHEP* **11** (2017) 095 [arXiv:1708.09408] [INSPIRE].

[34] K. Kannike, *Vacuum Stability Conditions From Copositivity Criteria*, *Eur. Phys. J.* **C 72** (2012) 2093 [arXiv:1205.3781] [INSPIRE].

[35] K.P. Hadeler, *On Copositive Matrices*, *Linear Algebra Appl.* **49** (1983) 79.

[36] W. Grimus, L. Lavoura, O.M. Ogreid and P. Osland, *A Precision constraint on multi-Higgs-doublet models*, *J. Phys.* **G 35** (2008) 075001 [arXiv:0711.4022] [INSPIRE].

[37] M. Maniatis, A. von Manteuffel, O. Nachtmann and F. Nagel, *Stability and symmetry breaking in the general two-Higgs-doublet model*, *Eur. Phys. J.* **C 48** (2006) 805 [hep-ph/0605184] [INSPIRE].

[38] I.F. Ginzburg and I.P. Ivanov, *Tree-level unitarity constraints in the most general 2HDM*, *Phys. Rev.* **D 72** (2005) 115010 [hep-ph/0508020] [INSPIRE].

[39] S. Kanemura and K. Yagyu, *Unitarity bound in the most general two Higgs doublet model*, *Phys. Lett.* **B 751** (2015) 289 [arXiv:1509.06060] [INSPIRE].

[40] I.P. Ivanov, *Minkowski space structure of the Higgs potential in 2HDM*, *Phys. Rev.* **D 75** (2007) 035001 [*Erratum ibid.* **D 76** (2007) 039902] [hep-ph/0609018] [INSPIRE].

[41] I.P. Ivanov and J.P. Silva, *Tree-level metastability bounds for the most general two Higgs doublet model*, *Phys. Rev.* **D 92** (2015) 055017 [arXiv:1507.05100] [INSPIRE].

[42] N.G. Deshpande and E. Ma, *Pattern of Symmetry Breaking with Two Higgs Doublets*, *Phys. Rev.* **D 18** (1978) 2574 [INSPIRE].

[43] K.G. Klimenko, *On Necessary and Sufficient Conditions for Some Higgs Potentials to Be Bounded From Below*, *Theor. Math. Phys.* **62** (1985) 58 [INSPIRE].

[44] P.M. Ferreira, R. Santos and A. Barroso, *Stability of the tree-level vacuum in two Higgs doublet models against charge or CP spontaneous violation*, *Phys. Lett.* **B 603** (2004) 219 [*Erratum ibid.* **B 629** (2005) 114] [hep-ph/0406231] [INSPIRE].

[45] F. Staub, *Reopen parameter regions in Two-Higgs Doublet Models*, *Phys. Lett.* **B 776** (2018) 407 [arXiv:1705.03677] [INSPIRE].

[46] L. Lavoura and J.P. Silva, *Fundamental CP-violating quantities in a* SU(2) × U(1) *model with many Higgs doublets*, *Phys. Rev.* **D 50** (1994) 4619 [hep-ph/9404276] [INSPIRE].

[47] A. Arhrib, *Phenomenology of 2HDM with a real singlet*, talk at *The Workshop on Multi-Higgs Models*, Lisbon, Portugal, 4–7 September 2018 [http://cftp.ist.utl.pt].

[48] I.P. Ivanov, M. Köpke and M. Mühlleitner, *Algorithmic Boundedness-From-Below Conditions for Generic Scalar Potentials*, *Eur. Phys. J.* **C 78** (2018) 413 [arXiv:1802.07976] [INSPIRE].

[49] G.T. Gilber, *Positive definite matrices and Sylvester's criterion*, *Am. Math. Monthly* **98** (1991) 44.

[50] X.-J. Xu, *Tree-level vacuum stability of two-Higgs-doublet models and new constraints on the scalar potential*, *Phys. Rev.* **D 95** (2017) 115019 [arXiv:1705.08965] [INSPIRE].